Noname manuscript No.
(will be inserted by the editor)

Uniquely solvable and energy stable decoupled numerical schemes for the Cahn-Hilliard-Navier-Stokes-Darcy-Boussinesq system

Wenbin Chen · Daozhi Han · Xiaoming Wang · Yichao Zhang

the date of receipt and acceptance should be inserted later

Abstract In this article we propose the Cahn-Hilliard-Navier-Stokes-Darcy-Boussinesq system that models thermal convection of two-phase flows in a fluid layer overlying a porous medium. Based on operator splitting and pressure stabilization we propose a family of fully decoupled numerical schemes such that the Navier-Stokes equations, the Darcy equations, the heat equation and the Cahn-Hilliard equation are solved independently at each time step, thus significantly reducing the computational cost. We show that

W. Chen and Y. Zhang are supported by the National Science Foundation of China (11671098, 91630309, 12071090). D. Han acknowledges support from NSF-DMS-1912715. X. Wang thanks support from NSFC11871159 and Guangdong Provincial Key Laboratory via 2019B030301001

W. Chen

School of Mathematical Sciences, Fudan University, Shanghai 200433, China

E-mail: wbchen@fudan.edu.cn

D. Han

Department of Mathematics and Statistics, Missouri University of Science and Technology, Rolla, MO 65409

E-mail: handaoz@mst.edu

X. Wang

Department of Mathematics, and SUSTech International Center for Mathematics, and National Center for Applied Mathematics Shenzhen, Southern University of Science and Technology, Shenzhen 518055, China

E-mail: wxm.math@outlook.com,

Y. Zhang

School of Mathematical Sciences, Fudan University, Shanghai 200433, China

E-mail: yichaozhang16@fudan.edu.cn

the schemes preserve the underlying energy law and hence are unconditionally long-time stable. Numerical results are presented to demonstrate the accuracy and stability of the algorithms.

Keywords phase field model · two-phase flow · convection · unconditional stability

Mathematics Subject Classification (2000) 35K61 · 76T99 · 76S05 · 76D07

1 Introduction

Many natural and engineering applications involve multiphase flows in superposed free flow and porous media. One such example is the mixing of surface water and shallow groundwater in the hyporheic zone–a region of sediment and porous space beneath and alongside a stream bed. Many important hydrodynamic and biogeochemical processes take place in this zone, and the hyporheic zone plays a major role in maintaining the self-purification function of streams, cf. [3]. Other applications in this context include contaminant transport in karst aquifers [41], oil recovery in petroleum engineering [19], water management in PEM fuel cell technology [43], and cardiovascular modeling and simulation [12].

The study of single phase flow in superposed fluid and porous media is usually pursued via either the Stokes-Darcy coupling or the Navier-Stokes-Darcy coupling [2, 6, 7, 8, 12, 17, 33]. The study of multiphase flow in the coupled domain is very challenging, and no sharp interface model is available to date. A hybrid of the sharp interface model in porous media and the diffuse interface model in the free flow is recently proposed in [5]. Based on Onsager's extremum principle and the diffuse interface formalism the Cahn-Hilliard-Stokes-Darcy system (CHSD) is systematically derived in [25] for two-phase flows in coupled conduit and porous media, cf. [27] for the well-posedness of the CHSD.

In many applications the free flow is necessarily governed by the Navier-Stokes equations as opposed to the Stokes equations employed in [5]. Furthermore, flows in hyporheic zone and in oil recovery are naturally non-isothermal [30]. In this article we propose the Cahn-Hilliard-Navier-Stokes-Darcy-Boussinesq (CHNSDB) system that models thermal convection of two-phase flows in a fluid layer overlying a porous medium. Non-isothermal effect is taken into account by the Boussinesq approximation and the suppressing of thermocapillary effects, which is suitable for most applications of multiphase flow in superposed fluid and porous media. We note that thermocapillary effect can be considered in the spirit of [22] if surface tension variation is significant. The CHNSDB model is shown to obey an energy law.

The CHNSDB model is a complex system that involves four coupled physical processes: the phase field model (the Cahn-Hilliard equation), the thermal conduction (the heat equation), fluid in free flow (the Navier-Stokes equations), and fluid flow in porous media (the Darcy system). In order to reduce the computation cost, we design numerical schemes that totally decouple the computation of the four processes at a time step. The main ideas are operator splitting and pressure stabilization that are inspired by [9, 10, 34, 42]. We establish the unconditional unique solvability and unconditional long-time stability of the algorithms. Numerical experiments are performed to verify the accuracy, the long-time stability, and the ability to capture convection cells of the proposed algorithms.

The design of energy law preserving numerical schemes are of great importance for solving phase field fluid models, owing to the stiffness associated with the diffusive interface (sharp transition in thin layers). Many approaches have been proposed in recent years, including the convex-concave splitting [4, 13, 18, 36], the stabilized linear approach [39], the Invariant Energy Quadratization (Lagrange multiplier) method [15, 20, 45, 46], and the Scalar Auxiliary Variable approach [37, 38]. Applications of these methods to phase field fluid models can be found in [11, 14, 21, 23, 24, 26, 28, 32, 40, 47] among many others.

The rest of the article is organized as follows. In Sec. 2 we introduce the CHNSDB model, establish the energy law, and introduce the weak formulation. We present the numerical algorithms and prove their unconditional unique solvability and long-time stability in Sec. 3. Numerical results are provided in Sec. 4. We conclude the article with some remarks in Sec. 5.

2 The mathematical model

Let us assume that the whole model is confined in a bounded connected domain $\Omega \in \mathbb{R}^d$ $(d = 2, 3)$ with sufficiently smooth boundary. The domain Ω is split into two non-overlapping regions Ω_c, Ω_m such that $\overline{\Omega} = \overline{\Omega}_c \cup \overline{\Omega}_m$ and $\Omega_c \cap \Omega_m = \emptyset$. Ω_c represents the conduit area where the fluids are subject to the Navier-Stokes equation, and Ω_m represents the porous media where Darcy flow dominates the region. We denote $\partial\Omega_c$ and $\partial\Omega_m$ the boundaries of Ω_c and Ω_m respectively, while both boundaries are assumed to be Lipschitz continuous. The interface between the two regions (i.e., $\partial\Omega_c \cap \partial\Omega_m$) is denoted by Γ_{cm}, on which $\mathbf{n}_{cm}$ denotes the unit normal to Γ_{cm} pointing from Ω_c to Ω_m. We also denote $\Gamma_c = \partial\Omega_c \backslash \Gamma_{cm}$ and $\Gamma_m = \partial\Omega_m \backslash \Gamma_{cm}$ with $\mathbf{n}_c, \mathbf{n}_m$ being the unit outer normals to Γ_c and Γ_m. On the interface Γ_{cm}, we denote

by $\{\boldsymbol{\tau}_i\}$ $(i = 1, ..., d-1)$ a local orthonormal basis for the tangent plane to Γ_{cm}. A two dimensional geometry is illustrated in Fig. 1.

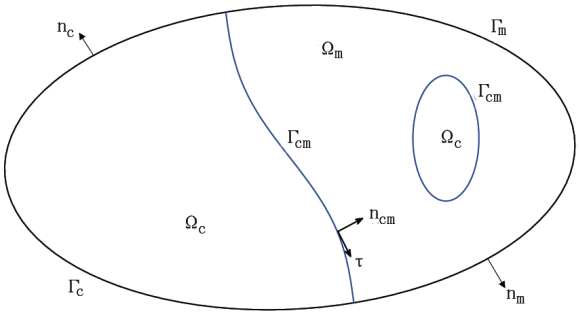

Fig. 1: A 2D illustration of the domain.

The subscript m (or c) represents the regions where the variables locate. m is for the matrix part of the Darcy system, and c is for the conduit part of the Navier-Stokes system. We denote by $\mathbf{u}$ the velocity of the whole fluid, φ the phase field function and T the overall temperature. We assume the following convention throughout the paper, that is, for $j \in \{c, m\}$

$$\mathbf{u}|_{\Omega_j} = \mathbf{u}_j, \quad \varphi|_{\Omega_j} = \varphi_j, \quad \mathrm{T}|_{\Omega_j} = \mathrm{T}_j.$$

This also applies to other functions and variables on the whole domain, such as μ, ν and κ, which will be introduced in the sequel.

2.1 The model and the energy law

Now let us consider the Cahn-Hilliard-Navier-Stokes-Darcy-Boussinesq(CHNSDB) system as follows:

$$\rho_0\Big(\partial_t\mathbf{u}_c + (\mathbf{u}_c\cdot\nabla)\mathbf{u}_c\Big) - \nabla\cdot\Big(2\nu(\varphi_c,\mathrm{T}_c)\mathbb{D}(\mathbf{u}_c)\Big) + \nabla P_c + \varphi_c\nabla\mu_c = -\rho_0\left(1-\alpha(\mathrm{T}_c-\mathrm{T}^*)\right)g\mathbf{z}, \quad \text{in } \Omega_c, \tag{2.1}$$

$$\frac{\rho_0}{\chi}\partial_t\mathbf{u}_m + \nu(\varphi_m,\mathrm{T}_m)\Pi^{-1}\mathbf{u}_m + \nabla P_m + \varphi_m\nabla\mu_m = -\rho_0\left(1-\alpha(\mathrm{T}_m-\mathrm{T}^*)\right)g\mathbf{z}, \quad \text{in } \Omega_m, \tag{2.2}$$

$$\nabla\cdot\mathbf{u}_j = 0, \quad \text{in } \Omega_j, \tag{2.3}$$

$$\partial_t\mathrm{T}_j + \mathbf{u}_j\cdot\nabla\mathrm{T}_j = \nabla\cdot\left(\kappa_j(\mathrm{T}_j)\nabla\mathrm{T}_j\right), \quad \text{in } \Omega_j, \tag{2.4}$$

$$\partial_t\varphi_j + \nabla\cdot(\mathbf{u}_j\varphi_j) = \mathrm{div}(\mathrm{M}(\varphi_j)\nabla\mu_j), \quad \text{in } \Omega_j, \tag{2.5}$$

$$\mu_j = \gamma[\frac{1}{\epsilon}(\varphi_j^3 - \varphi_j) - \epsilon\Delta\varphi_j], \quad \text{in } \Omega_j, \tag{2.6}$$

where $j \in \{c, m\}$ and $\mathbb{D}(\mathbf{u}_c)$ is given by

$$\mathbb{D}(\mathbf{u}_c) = \frac{1}{2}(\nabla\mathbf{u}_c + \nabla^T\mathbf{u}_c), \tag{2.7}$$

denoting the rate of strain tensor. Here ρ_0 is a constant representing the approximation of the fluid density, α is the thermal expansion coefficient and T^* is a fixed temperature, g is the gravitational acceleration, $\mathbf{z}$ is the unit vector pointing in the inverse direction of gravity, M is a non-negative smooth function which denotes the mobility, χ is the porosity and $\mathit{\Pi}$ is the permeability matrix with size of $d \times d$, ν is the dynamic viscosity depending on phase field function φ and temperature T, κ is thermal diffusivity of the fluid mixture and is dependent on temperature T, μ is the chemical potential and γ is a positive parameter related to the surface tension. Moreover, we assume that the viscosity ν, thermal diffusivity κ and mobility M are suitable functions such that $0 < \bar{c} \leq \nu, \kappa, \mathrm{M} \leq \bar{C}$ for positive constants $\bar{c}$ and $\bar{C}$.

The CHNSDB system is subject to the following boundary and interface conditions.

Boundary conditions on $\mathit{\Gamma}_c$ and $\mathit{\Gamma}_m$:

$$\mathbf{u}_c = \mathbf{0}, \quad \frac{\partial \mathrm{T}_c}{\partial \mathbf{n}_c} = \frac{\partial \varphi_c}{\partial \mathbf{n}_c} = \frac{\partial \mu_c}{\partial \mathbf{n}_c} = 0, \quad \text{on } \mathit{\Gamma}_c, \tag{2.8}$$

$$\mathbf{u}_m \cdot \mathbf{n}_m = 0, \quad \frac{\partial \mathrm{T}_m}{\partial \mathbf{n}_m} = \frac{\partial \varphi_m}{\partial \mathbf{n}_m} = \frac{\partial \mu_m}{\partial \mathbf{n}_m} = 0, \quad \text{on } \mathit{\Gamma}_m. \tag{2.9}$$

Interface conditions on $\mathit{\Gamma}_{cm}$:

$$\varphi_m = \varphi_c, \quad \frac{\partial \varphi_m}{\partial \mathbf{n}_{cm}} = \frac{\partial \varphi_c}{\partial \mathbf{n}_{cm}}, \quad \text{on } \mathit{\Gamma}_{cm}, \tag{2.10}$$

$$\mu_m = \mu_c, \quad \mathrm{M}(\varphi_m)\frac{\partial \mu_m}{\partial \mathbf{n}_{cm}} = \mathrm{M}(\varphi_c)\frac{\partial \mu_c}{\partial \mathbf{n}_{cm}}, \quad \text{on } \mathit{\Gamma}_{cm}, \tag{2.11}$$

$$\mathrm{T}_m = \mathrm{T}_c, \quad \kappa_m \frac{\partial \mathrm{T}_m}{\partial \mathbf{n}_{cm}} = \kappa_c \frac{\partial \mathrm{T}_c}{\partial \mathbf{n}_{cm}}, \quad \text{on } \mathit{\Gamma}_{cm}, \tag{2.12}$$

$$\mathbf{u}_m \cdot \mathbf{n}_{cm} = \mathbf{u}_c \cdot \mathbf{n}_{cm}, \quad \text{on } \mathit{\Gamma}_{cm}, \tag{2.13}$$

$$-2\nu(\varphi_c)\mathbf{n}_{cm} \cdot (\mathbb{D}(\mathbf{u}_c)\mathbf{n}_{cm}) + P_c + \frac{1}{2}\rho_0|\mathbf{u}_c|^2 = P_m, \quad \text{on } \mathit{\Gamma}_{cm}, \tag{2.14}$$

$$-\tau_i \cdot (\mathbb{D}(\mathbf{u}_c)\mathbf{n}_{cm}) = \frac{\alpha_{BJSJ}}{2\sqrt{\mathrm{trace}(\mathit{\Pi})}}\tau_i \cdot \mathbf{u}_c, \quad i = 1, \ldots, d-1, \text{on } \mathit{\Gamma}_{cm}, \tag{2.15}$$

where α_{BJSJ} is a parameter in the Beavers-Joseph-Saffman-Jones(BJSJ) condition. Here α_{BJSJ} is assumed to be a non-negative constant for simplicity.

We assert that for all $T \geq 0$, $\overline{\mathrm{T}}$ (the mean value of T) is a constant for our CHNSDB system. For the PDE solution there holds

$$\begin{aligned}\frac{d}{dt}\left(\int_\Omega \mathrm{T}dx\right) &= \int_\Omega \partial_t \mathrm{T}dx = \sum_{j\in\{c,m\}}\int_{\Omega_j}\Big(\nabla\cdot(\kappa_j(\mathrm{T}_j)\nabla\mathrm{T}_j) - \mathbf{u}_j\cdot\nabla\mathrm{T}_j\Big)dx \\ &= \sum_{j\in\{c,m\}}\left(\int_{\Gamma_j}\kappa(\mathrm{T}_j)\frac{\partial\mathrm{T}_j}{\partial\mathbf{n}_j}dx + \int_{\Omega_j}\left[\mathrm{T}_j\nabla\cdot\mathbf{u}_j - \nabla\cdot(\mathbf{u}_j\mathrm{T}_j)\right]dx\right) \\ &= -\sum_{j\in\{c,m\}}\int_{\Gamma_j}\mathrm{T}_j\mathbf{u}_j\cdot\mathbf{n}_j dx = 0.\end{aligned}$$

Additionally, we choose z to be the ordinate of the axis parallel to $\mathbf{z}$ satisfying $\nabla z = \mathbf{z}$, then for $j \in \{c, m\}$ there holds

$$\begin{aligned}-\rho_0\left(1-\alpha(\mathrm{T}_j-\mathrm{T}^*)\right)g\mathbf{z} &= \alpha\rho_0 g(\mathrm{T}_j-\overline{\mathrm{T}})\mathbf{z} - \rho_0\left(1-\alpha(\overline{\mathrm{T}}-\mathrm{T}^*)\right)g\mathbf{z} \\ &= \alpha\rho_0 g(\mathrm{T}_j-\overline{\mathrm{T}})\mathbf{z} - \nabla\left(\rho_0\left(1-\alpha(\overline{\mathrm{T}}-\mathrm{T}^*)\right)gz\right).\end{aligned}$$

Hence the second term above can be combined with ∇P_j ($j \in \{c, m\}$) on the left hand side of the fluid equation, that is to set

$$\widetilde{P}_j = P_j + \rho_0\left(1-\alpha(\overline{\mathrm{T}}-\mathrm{T}^*)\right)gz, \quad j\{c,m\},$$

and replace P_j with $\widetilde{P}_j$. Notice that $\rho_0\left(1-\alpha(\overline{\mathrm{T}}-\mathrm{T}^*)\right)gz$ is a constant so that the interface condition (2.14) still holds for $\widetilde{P}_j$. By continuing to use P_j instead of $\widetilde{P}_j$ for simplicity the PDE system (2.1)–(2.6) is equivalent to the following system with $j \in \{c, m\}$:

$$\rho_0\Big(\partial_t\mathbf{u}_c + (\mathbf{u}_c\cdot\nabla)\mathbf{u}_c\Big) - \nabla\cdot\Big(2\nu(\varphi_c,\mathrm{T}_c)\mathbb{D}(\mathbf{u}_c)\Big) + \nabla P_c + \varphi_c\nabla\mu_c = \alpha\rho_0 g(\mathrm{T}_c-\overline{\mathrm{T}})\mathbf{z}, \quad \text{in } \Omega_c, \tag{2.16}$$

$$\frac{\rho_0}{\chi}\partial_t\mathbf{u}_m + \nu(\varphi_m,\mathrm{T}_m)\Pi^{-1}\mathbf{u}_m + \nabla P_m + \varphi_m\nabla\mu_m = \alpha\rho_0 g(\mathrm{T}_m-\overline{\mathrm{T}})\mathbf{z}, \quad \text{in } \Omega_m, \tag{2.17}$$

$$\nabla\cdot\mathbf{u}_j = 0, \quad \text{in } \Omega_j, \tag{2.18}$$

$$\partial_t\mathrm{T}_j + \mathbf{u}_j\cdot\nabla\mathrm{T}_j = \nabla\cdot\left(\kappa_j(\mathrm{T}_j)\nabla\mathrm{T}_j\right), \quad \text{in } \Omega_j, \tag{2.19}$$

$$\partial_t\varphi_j + \nabla\cdot(\mathbf{u}_j\varphi_j) = \mathrm{div}(\mathrm{M}(\varphi_j)\nabla\mu_j), \quad \text{in } \Omega_j, \tag{2.20}$$

$$\mu_j = \gamma[\frac{1}{\epsilon}(\varphi_j^3-\varphi_j) - \epsilon\Delta\varphi_j], \quad \text{in } \Omega_j. \tag{2.21}$$

It is important to declare that the CHNSDB system (2.8)-(2.21) obeys an energy law. Here we need to introduce some constants. Set λ as the upper bound of the largest eigenvalue of Π. Let $C_p, C_k > 0$ be the coefficients such that

$$\left\|\mathrm{T}-\overline{\mathrm{T}}\right\|^2_{L^2(\Omega)} \leq C_p\left\|\nabla\mathrm{T}\right\|^2_{L^2(\Omega)}, \qquad \left\|\mathbf{u}_c\right\|^2_{L^2(\Omega_c)} \leq C_k\left\|\mathbb{D}(\mathbf{u}_c)\right\|^2_{L^2(\Omega_c)} \tag{2.22}$$

hold for all $\mathrm{T} \in H^1(\Omega), \mathbf{u}_c \in H^1(\Omega_c)$. For any constant A such that

$$A \geq \max\{\frac{C_p C_k (\alpha\rho_0 g)^2}{8\bar{c}^2}, \frac{C_p \lambda (\alpha\rho_0 g)^2}{4\bar{c}^2}\}, \tag{2.23}$$

we define the total energy of the system as follows:

$$\mathcal{E}_A(t) := \int_{\Omega_c} \frac{\rho_0}{2}|\mathbf{u}_c|^2 dx + \int_{\Omega_m} \frac{\rho_0}{2\chi}|\mathbf{u}_m|^2 dx + A\int_\Omega \frac{1}{2}\mathrm{T}^2 dx + \gamma\int_\Omega \left[\frac{\epsilon}{2}|\nabla\varphi|^2 + \frac{1}{\epsilon}F(\varphi)\right] dx, \tag{2.24}$$

where $F(\varphi) = \frac{1}{4}(\varphi^2-1)^2$. The last integral term is the free energy function

$$E(\varphi) = \gamma\int_\Omega \left[\frac{1}{\epsilon}F(\varphi) + \frac{\epsilon}{2}|\nabla\varphi|^2\right] dx.$$

It is known from thermodynamics that without external differential heating the total energy of the system decays in time. The CHNSDB system obeys this principle. Let $(\mathbf{u}_m, \mathbf{u}_c, \mathrm{T}, \varphi)$ be a sufficiently smooth solution to (2.8)-(2.21), then for all $t \geq 0$, $(\mathbf{u}_m, \mathbf{u}_c, \mathrm{T}, \varphi)$ satisfies the following energy law:

Lemma 1 *For constant A that satisfies* (2.23)*, the solution to the PDE system* (2.8)-(2.21) *satisfies*

$$\frac{d}{dt}\mathcal{E}_A(t) \leq 0, \qquad \forall t \geq 0. \tag{2.25}$$

Proof Notice that $\mathbf{z}$ is a unit vector, then by the Cauchy-Schwarz inequality, (2.22) and (2.23) we have

$$\begin{aligned}\int_{\Omega_c} \alpha\rho_0 g(\mathrm{T}_c - \overline{\mathrm{T}})\mathbf{z}\cdot\mathbf{u}_c dx &\leq \int_{\Omega_c}\left(\frac{C_k(\alpha\rho_0 g)^2}{8\nu(\varphi_c,\mathrm{T}_c)}(\mathrm{T}_c-\overline{\mathrm{T}})^2 + \frac{2\nu(\varphi_c,\mathrm{T}_c)}{C_k}|\mathbf{u}_c|^2\right) dx \\ &\leq \int_{\Omega_c}\left(\frac{\kappa(\mathrm{T_c})A}{C_p}(\mathrm{T}_c-\overline{\mathrm{T}})^2 + 2\nu(\varphi_c,\mathrm{T}_c)|\mathbb{D}(\mathbf{u}_c)|^2\right) dx. \end{aligned}\tag{2.26}$$

Since

$$\left|\Pi^{1/2}\mathbf{z}\right|^2 = \mathbf{z}^\top \Pi \mathbf{z} \leq \max_{|\mathbf{v}|=1} \mathbf{v}^\top \Pi \mathbf{v} = \lambda_{\max}(\Pi) \leq \lambda, \tag{2.27}$$

then

$$\begin{aligned}\int_{\Omega_m} \alpha\rho_0 g(\mathrm{T}_m - \overline{\mathrm{T}})\mathbf{z}\cdot\mathbf{u}_m dx &= \int_{\Omega_m} \alpha\rho_0 g(\mathrm{T}_m-\overline{\mathrm{T}})\Pi^{1/2}\mathbf{z}\cdot\Pi^{-1/2}\mathbf{u}_m dx \\ &\leq \int_{\Omega_m}\left(\frac{(\alpha\rho_0 g)^2}{4\nu(\varphi_m,\mathrm{T}_m)}(\mathrm{T}_m-\overline{\mathrm{T}})^2\left|\Pi^{1/2}\mathbf{z}\right|^2 + \nu(\varphi_m,\mathrm{T}_m)\left|\Pi^{-1/2}\mathbf{u}_m\right|^2\right) dx \\ &\leq \int_{\Omega_m}\left(\frac{\lambda(\alpha\rho_0 g)^2}{4\nu(\varphi_m,\mathrm{T}_m)}(\mathrm{T}_m-\overline{\mathrm{T}})^2 + \nu(\varphi_m,\mathrm{T}_m)\left|\Pi^{-1/2}\mathbf{u}_m\right|^2\right) dx \\ &\leq \int_{\Omega_m}\left(\frac{\kappa(\mathrm{T_m})A}{C_p}(\mathrm{T}_m-\overline{\mathrm{T}})^2 + \nu(\varphi_m,\mathrm{T}_m)\left|\Pi^{-1/2}\mathbf{u}_m\right|^2\right) dx. \end{aligned}\tag{2.28}$$

Inequalities (2.26) and (2.28) imply

$$\int_{\Omega_c} \alpha\rho_0 g(\mathrm{T}_c-\overline{\mathrm{T}})\mathbf{z}\cdot\mathbf{u}_c dx + \int_{\Omega_m} \alpha\rho_0 g(\mathrm{T}_m-\overline{\mathrm{T}})\mathbf{z}\cdot\mathbf{u}_m dx$$

$$\leq \int_{\Omega} \frac{\kappa(\mathrm{T})A}{C_p}(\mathrm{T}-\overline{\mathrm{T}})^2 dx + \int_{\Omega_c} 2\nu(\varphi_c,\mathrm{T}_c)|\mathbb{D}(\mathbf{u}_c)|^2 dx + \int_{\Omega_m} \nu(\varphi_m,\mathrm{T}_m)\left|\Pi^{-1/2}\mathbf{u}_m\right|^2 dx$$
$$\leq \int_{\Omega} \kappa(\mathrm{T})A|\nabla \mathrm{T}|^2 dx + \int_{\Omega_c} 2\nu(\varphi_c,\mathrm{T}_c)|\mathbb{D}(\mathbf{u}_c)|^2 dx + \int_{\Omega_m} \nu(\varphi_m,\mathrm{T}_m)\left|\Pi^{-1/2}\mathbf{u}_m\right|^2 dx. \tag{2.29}$$

A standard energy estimate to (2.8)-(2.21) then gives

$$\begin{aligned}
\frac{d}{dt}\mathcal{E}(t) =& -\int_{\Omega_c} 2\nu(\varphi_c,\mathrm{T}_c)|\mathbb{D}(\mathbf{u}_c)|^2 dx - \int_{\Omega_m} \nu(\varphi_m,\mathrm{T}_m)\left|\Pi^{-1/2}\mathbf{u}_m\right|^2 dx - \int_{\Omega} \kappa(\mathrm{T})A|\nabla \mathrm{T}|^2 dx \\
&- \int_{\Omega} \mathrm{M}(\varphi)|\nabla \mu(\varphi)|^2 dx - \int_{\Gamma_{cm}} \alpha_{BJSJ}\frac{\nu(\varphi,\mathrm{T})}{\sqrt{\mathrm{trace}(\Pi)}}\sum_{i=1}^{d-1}|\tau_i\cdot\mathbf{u}_c|^2 dS \\
&+ \int_{\Omega_c} \alpha\rho_0 g(\mathrm{T}_c-\overline{\mathrm{T}})\mathbf{z}\cdot\mathbf{u}_c dx + \int_{\Omega_m} \alpha\rho_0 g(\mathrm{T}_m-\overline{\mathrm{T}})\mathbf{z}\cdot\mathbf{u}_m dx \\
\leq& -\int_{\Omega_c} 2\nu(\varphi_c,\mathrm{T}_c)|\mathbb{D}(\mathbf{u}_c)|^2 dx - \int_{\Omega_m} \nu(\varphi_m,\mathrm{T}_m)\left|\Pi^{-1/2}\mathbf{u}_m\right|^2 dx - \int_{\Omega} \kappa(\mathrm{T})A|\nabla \mathrm{T}|^2 dx \\
&- \int_{\Omega} \mathrm{M}(\varphi)|\nabla \mu(\varphi)|^2 dx - \int_{\Gamma_{cm}} \alpha_{BJSJ}\frac{\nu(\varphi,\mathrm{T})}{\sqrt{\mathrm{trace}(\Pi)}}\sum_{i=1}^{d-1}|\tau_i\cdot\mathbf{u}_c|^2 dS \\
&+ \int_{\Omega} \kappa(\mathrm{T})A|\nabla \mathrm{T}|^2 dx + \int_{\Omega_c} 2\nu(\varphi_c,\mathrm{T}_c)|\mathbb{D}(\mathbf{u}_c)|^2 dx + \int_{\Omega_m} \nu(\varphi_m,\mathrm{T}_m)\left|\Pi^{-1/2}\mathbf{u}_m\right|^2 dx \\
=& -\int_{\Omega} \mathrm{M}(\varphi)|\nabla \mu(\varphi)|^2 dx - \int_{\Gamma_{cm}} \alpha_{BJSJ}\frac{\nu(\varphi,\mathrm{T})}{\sqrt{\mathrm{trace}(\Pi)}}\sum_{i=1}^{d-1}|\tau_i\cdot\mathbf{u}_c|^2 dS \\
\leq& 0.
\end{aligned} \tag{2.30}$$

This completes the proof. □

2.2 The weak formulation

We introduce the following spaces

$$\mathbf{H}(\mathrm{div};\Omega_j) := \{\mathbf{w}\in\mathbf{L}^2(\Omega_j) \mid \nabla\cdot\mathbf{w}\in\mathbf{L}^2(\Omega_j)\}, \qquad j\in\{c,m\},$$
$$\mathbf{H}_{c,0} := \{\mathbf{w}\in\mathbf{H}^1(\Omega_c) \mid \mathbf{w}=\mathbf{0} \text{ on } \Gamma_c\},$$
$$\mathbf{H}_{c,\mathrm{div}} := \{\mathbf{w}\in\mathbf{H}_{c,0} \mid \nabla\cdot\mathbf{w}=0\},$$
$$\mathbf{H}_{m,0} := \{\mathbf{w}\in\mathbf{H}(\mathrm{div};\Omega_m) \mid \mathbf{w}\cdot\mathbf{n}_m=0 \text{ on } \Gamma_m\},$$
$$\mathbf{H}_{m,\mathrm{div}} := \{\mathbf{w}\in\mathbf{H}_{m,0} \mid \nabla\cdot\mathbf{w}=0\},$$
$$X_m := H^1(\Omega_m)\cap L_0^2(\Omega_m).$$

Here $L_0^2(\Omega_m)$ is a subspace of L^2 whose elements are of mean zero. We denote $(\cdot,\cdot)_c$, $(\cdot,\cdot)_m$ the inner products on the spaces $L^2(\Omega_c)$, $L^2(\Omega_m)$, respectively (also for the corresponding vector spaces). The inner product

on $L^2(\Omega)$ is simply denoted by $(\cdot,\cdot)$. Then it is clear that

$$(u,v)=(u_m,v_m)_m+(u_c,v_c)_c,\quad \|u\|^2_{L^2(\Omega)}=\|u_m\|^2_{L^2(\Omega_m)}+\|u_c\|^2_{L^2(\Omega_c)},$$

where $u_m:=u|_{\Omega_m}$ and $u_c:=u|_{\Omega_c}$. We will suppress the dependence on the domain in the L^2 norm if there is no ambiguity. We also denote H' the dual space of H with the duality induced by the L^2 inner product. The weak formulation of the CHNSDB system in three dimension is given by the following definition. The formulation in two dimension is defined similarly.

Definition 1 Suppose that $d=3$ and $\mathcal{T}>0$ is arbitrary (distinguish time $\mathcal{T}$ from temperature T carefully). We consider the initial data $\varphi_0\in H^1(\Omega),\mathbf{u}_c(0)\in\mathbf{H}_{c,\mathrm{div}},\mathbf{u}_m(0)\in\mathbf{H}_{m,\mathrm{div}},\mathrm{T}_0\in H^1(\Omega)$. The functions $(\mathbf{u}_c,P_c,\mathbf{u}_m,P_m,\mathrm{T},\varphi,\mu)$ with the following properties

$$\mathbf{u}_c\in L^\infty(0,\mathcal{T};\mathbf{L^2}(\Omega_c))\cap L^2(0,\mathcal{T};\mathbf{H}_{c,0}),\ \tfrac{\partial\mathbf{u}_c}{\partial t}\in L^{\frac43}(0,\mathcal{T};(\mathbf{H}_{c,0})'),\tag{2.31}$$

$$\mathbf{u}_m\in L^\infty(0,\mathcal{T};\mathbf{L^2}(\Omega_m))\cap L^2(0,\mathcal{T};\mathbf{H}_{m,0}),\ \tfrac{\partial\mathbf{u}_m}{\partial t}\in L^{\frac43}(0,\mathcal{T};(\mathbf{H}_{m,0})'),\tag{2.32}$$

$$P_c\in L^{\frac43}(0,\mathcal{T};L^2(\Omega_c)),\quad P_m\in L^{\frac43}(0,\mathcal{T};X_m),\tag{2.33}$$

$$\mathrm{T}\in L^\infty(0,\mathcal{T};L^2(\Omega))\cap L^2(0,\mathcal{T};H^1(\Omega)),\mathrm{T}_t\in L^2(0,\mathcal{T};(H^1(\Omega))'),\tag{2.34}$$

$$\varphi\in L^\infty(0,\mathcal{T};H^1(\Omega))\cap L^2(0,\mathcal{T};H^3(\Omega)),\varphi_t\in L^2(0,\mathcal{T};(H^1(\Omega))'),\tag{2.35}$$

$$\mu\in L^2(0,\mathcal{T};H^1(\Omega)),\tag{2.36}$$

is called a finite energy weak solution of the CHNSDB system (2.8)–(2.21), if the following conditions are satisfied:

(1) For any $\mathbf{v}_c\in\mathbf{H}_{c,0}$ and $q_c\in L^2(\Omega_c)$,

$$\begin{aligned}&\rho_0\langle\partial_t\mathbf{u}_c,\mathbf{v}_c\rangle_c+\rho_0\widetilde{\mathrm{B}}_c(\mathbf{u}_c,\mathbf{u}_c,\mathbf{v}_c)+2\left(\nu(\varphi_c,\mathrm{T}_c)\mathbb{D}(\mathbf{u}_c),\mathbb{D}(\mathbf{v}_c)\right)_c-(P_c,\nabla\cdot\mathbf{v}_c)_c\\&+\sum_{i=1}^{d-1}\alpha_{BJSJ}\int_{\Gamma_{cm}}\frac{\nu(\varphi_m)}{\sqrt{\mathrm{trace}(\Pi)}}(\mathbf{u}_c\cdot\boldsymbol{\tau}_i)(\mathbf{v}_c\cdot\boldsymbol{\tau}_i)dS+\int_{\Gamma_{cm}}P_m(\mathbf{v}_c\cdot\mathbf{n}_{cm})dS\\&+(\nabla\cdot\mathbf{u}_c,q_c)_c+(\varphi_c\nabla\mu(\varphi_c),\mathbf{v}_c)_c=(\alpha\rho_0 g(\mathrm{T}_c-\overline{\mathrm{T}})\mathbf{z},\mathbf{v}_c)_c,\end{aligned}\tag{2.37}$$

where

$$\widetilde{\mathrm{B}}_c(\mathbf{u},\mathbf{v},\mathbf{w})=\frac12\int_{\Omega_c}\Big((\mathbf{u}\cdot\nabla\mathbf{v})\mathbf{w}-(\mathbf{u}\cdot\nabla\mathbf{w})\mathbf{v}\Big)dx+\frac12\int_{\Gamma_{cm}}\Big((\mathbf{v}\cdot\mathbf{w})(\mathbf{u}\cdot\mathbf{n}_{cm})-(\mathbf{u}\cdot\mathbf{v})(\mathbf{w}\cdot\mathbf{n}_{cm})\Big)dS.\tag{2.38}$$

(2) For any $\mathbf{v}_m\in\mathbf{H}_{m,0}$ and $q_m\in H^1(\Omega_m)$,

$$\frac{\rho_0}{\chi}\langle\partial_t\mathbf{u}_m,\mathbf{v}_m\rangle_m+(\nu(\varphi_m,\mathrm{T}_m)\Pi^{-1}\mathbf{u}_m,\mathbf{v}_m)_m+(\nabla P_m,\mathbf{v}_m)_m-(\mathbf{u}_m,\nabla q_m)_m$$

$$+(\varphi_m\nabla\mu(\varphi_m),\mathbf{v}_m)_m-\int_{\Gamma_{cm}}\mathbf{u}_c\cdot\mathbf{n}_{cm}q_m\,ds=(\alpha\rho_0 g(\mathrm{T}_m-\overline{\mathrm{T}})\mathbf{z},\mathbf{v}_m)_m. \tag{2.39}$$

(3) For any $W\in H^1(\Omega)$,

$$\langle\partial_t\mathrm{T},W\rangle+\mathrm{B}(\mathbf{u},\mathrm{T},W)+(\kappa(\mathrm{T})\nabla\mathrm{T},\nabla W)=0, \tag{2.40}$$

where

$$\mathrm{B}(\mathbf{u},v,w)=\frac{1}{2}\int_\Omega\Big(\mathbf{u}\cdot(w\nabla v)-\mathbf{u}\cdot(v\nabla w)\Big)dx. \tag{2.41}$$

(4) For any $v,\phi\in H^1(\Omega)$,

$$\langle\partial_t\varphi,v)+(\mathrm{M}(\varphi)\nabla\mu(\varphi),\nabla v)-(\mathbf{u}\varphi,\nabla v)=0, \tag{2.42}$$

$$\gamma\left[\frac{1}{\epsilon}(f(\varphi),\phi)+\epsilon(\nabla\varphi,\nabla\phi)\right]-(\mu(\varphi),\phi)=0. \tag{2.43}$$

(5) $\varphi|_{t=0}=\varphi_0(x),\mathrm{T}|_{t=0}=\mathrm{T}_0(x),\mathbf{u}_c|_{t=0}=\mathbf{u}_c(0),\mathbf{u}_m|_{t=0}=\mathbf{u}_m(0)$.

Here we introduce another trilinear term

$$\mathrm{B}_c(\mathbf{u},\mathbf{v},\mathbf{w})=\frac{1}{2}\int_{\Omega_c}\Big((\mathbf{u}\cdot\nabla\mathbf{v})\mathbf{w}-(\mathbf{u}\cdot\nabla\mathbf{w})\mathbf{v}\Big)dx+\frac{1}{2}\int_{\Gamma_{cm}}\Big((\mathbf{u}\cdot\mathbf{w})(\mathbf{v}\cdot\mathbf{n}_{cm})-(\mathbf{u}\cdot\mathbf{v})(\mathbf{w}\cdot\mathbf{n}_{cm})\Big)dS. \tag{2.44}$$

We remark that $\mathrm{B}_c(\mathbf{u},\mathbf{v},\mathbf{w})$ is antisymmetric with respect to $\mathbf{v}$ and $\mathbf{w}$. Moreover, $\widetilde{\mathrm{B}}_c(\mathbf{u},\mathbf{v},\mathbf{w})=\mathrm{B}_c(\mathbf{u},\mathbf{v},\mathbf{w})$ when $\mathbf{u}=\mathbf{v}$. We will replace $\widetilde{\mathrm{B}}_c(\mathbf{u},\mathbf{v},\mathbf{w})$ with $\mathrm{B}_c(\mathbf{u},\mathbf{v},\mathbf{w})$ in the numerical scheme later. We note that the two trilinear terms $\mathrm{B}_c(\mathbf{u},\mathbf{v},\mathbf{w})$ and $\mathrm{B}(\mathbf{u},v,w)$ are different in the integral domains, the presence of integrals along domain interface, as well as the variables (vector vs scalar). In particular, $\mathrm{B}(\mathbf{u},v,w)$ in the heat equation (2.40) has an implied interfacial integral term $\frac{1}{2}\int_{\Gamma_{cm}}v(\mathbf{u}_c-\mathbf{u}_m)\cdot(w\mathbf{n}_{cm})dS$ which is equal to zero because of the interface condition (2.13) when $\mathbf{u}$ is the exact solution to the CHNSDB problem.

We also comment that the mean zero quality is only required in the definition of the space for P_m. Once P_m is uniquely determined, P_c is then also uniquely determined due to the interface boundary condition (2.14). We refer to [27] for the study of the existence of such a weak solution for a similar problem. For the weak solution we also have $\overline{\mathrm{T}}\equiv C$ due to the following estimate,

$$\begin{aligned}\frac{d}{dt}\left(\int_\Omega\mathrm{T}dx\right)&=\int_\Omega\partial_t\mathrm{T}dx=-\mathrm{B}(\mathbf{u},\mathrm{T},1)=-\frac{1}{2}\sum_{j\in\{c,m\}}\int_{\Omega_j}\mathbf{u}_j\cdot\nabla\mathrm{T}_j dx\\&=-\frac{1}{2}\left(\int_{\Gamma_{cm}}\mathbf{u}_c\cdot\mathbf{n}_{cm}\mathrm{T}_c dS-\int_{\Omega_c}\mathrm{T}_c\nabla\cdot\mathbf{u}_c dx-\int_{\Gamma_{cm}}\mathbf{u}_c\cdot\mathbf{n}_{cm}\mathrm{T}_m dx\right)\\&=-\frac{1}{2}\int_{\Gamma_{cm}}\mathbf{u}_c\cdot\mathbf{n}_{cm}(\mathrm{T}_c-\mathrm{T}_m)dx=0.\end{aligned} \tag{2.45}$$

3 Numerical schemes

Let $\tau > 0$ be the time step and $K = [\mathcal{T}/\tau]$. Set $t^k = k\tau$ for $0 \le k \le K$. Let Ω_c^h and Ω_m^h be the quasi-uniform triangulation of the domain Ω_c and Ω_m with mesh size h respectively. We assume that Ω_c^h and Ω_m^h coincide on the interface Γ_{cm}. Then $\Omega^h := \Omega_c^h \cup \Omega_m^h$ forms a triangulation of the whole domain Ω. Let $P_r(\mathcal{K})$ be the space of polynomials of degree equal to or less than r on triangle $\mathcal{K} \in \Omega^h$. Then Y_h refers to the finite element approximation of $H^1(\Omega)$ based on the triangulation Ω^h, such as

$$Y_h = \{v_h \in C(\bar{\Omega}) \big| v_h|_K \in P_r(\mathcal{K}), \forall \mathcal{K} \in \Omega_h\}.$$

Denote by $\mathbf{X}_c^h$ and M_c^h the finite element approximation of $\mathbf{H}_{c,0}$ and $L^2(\Omega_c)$ for the Navier-Stokes velocity and pressure respectively. We assume that $\mathbf{X}_c^h$ and M_c^h satisfy the inf-sup condition, or so-called LBB condition, that

$$\sup_{\mathbf{v}_h \in \mathbf{X}_c^h} \frac{(\nabla \cdot \mathbf{v}_h, q_h)_c}{\|\mathbf{v}_h\|_{H^1}} \ge c\|q_h\|_{L^2}, \quad \forall q_h \in M_c^h. \tag{3.1}$$

We point out that the classical Taylor-Hood finite element spaces and the Mini finite element spaces are normally used for $\mathbf{X}_c^h$ and M_c^h [16]. Similarly, we define $\mathbf{X}_m^h, M_m^h$ to be the finite element spaces of $\mathbf{H}_{m,0}, X_m$ for Darcy velocity and pressure respectively. In addition, we assume $\mathbf{X}_m^h$ and M_m^h satisfy a non-standard inf-sup condition such that

$$\sup_{\mathbf{v}_h \in \mathbf{X}_m^h} \frac{(\mathbf{v}_h, \nabla q_h)_m}{\|\mathbf{v}_h\|_{L^2}} \ge c\|q_h\|_{L^2}, \quad \forall q_h \in M_m^h. \tag{3.2}$$

The condition above can be supported by Taylor-Hood finite element spaces.

3.1 Energy stable fully decoupled numerical schemes

Now we are ready to discuss our unconditionally stable numerical schemes that fully decouple phase-field system (Cahn-Hilliard), heat equation and two different fluid systems (Navier-Stokes and Darcy) during the computation. We first arrange some notations here. δ_τ denotes the difference quotient operator such that $\delta_\tau \varphi_h^{k+1} = \frac{\varphi_h^{k+1} - \varphi_h^k}{\tau}$, and $f(\varphi_h^{k+1}, \varphi_h^k) = (\varphi_h^{k+1})^3 - \varphi_h^k$. The intermediate velocity $\overline{\mathbf{u}}_h^{k+1}$ is defined as

$$\overline{\mathbf{u}}^{k+1} = \begin{cases} \overline{\mathbf{u}}_{m,h}^{k+1}, & x \in \Omega_m, \\ \\ \overline{\mathbf{u}}_{c,h}^{k+1}, & x \in \Omega_c, \end{cases} \tag{3.3}$$

where $\overline{\mathbf{u}}_{m,h}^{k+1}$ and $\overline{\mathbf{u}}_{c,h}^{k+1}$ are defined by the equations below:

$$\frac{\rho_0}{\chi}\frac{\overline{\mathbf{u}}_{m,h}^{k+1}-\mathbf{u}_{m,h}^{k}}{\tau}+\varphi_{m,h}^{k}\nabla\mu_{m,h}^{k+1}=0, \tag{3.4}$$

$$\rho_0\frac{\overline{\mathbf{u}}_{c,h}^{k+1}-\mathbf{u}_{c,h}^{k}}{\tau}+\varphi_{c,h}^{k}\nabla\mu_{c,h}^{k+1}=0. \tag{3.5}$$

Additionally, for all $\mathbf{u}_{c,h},\mathbf{v}_{c,h}\in\mathbf{X}_c^h$, $P_{c,h},q_{c,h}\in M_c^h$ and $0\le k\le K$, we denote

$$\begin{aligned}a_c^k(\mathbf{u}_{c,h},\mathbf{v}_{c,h})&=2\left(\nu(\varphi_{c,h}^k,\mathrm{T}_{c,h}^k)\mathbb{D}(\mathbf{u}_{c,h}),\mathbb{D}(\mathbf{v}_{c,h})\right)_c\\&\quad+\sum_{i=1}^{d-1}\int_{\Gamma_{cm}}\alpha_{BJSJ}\frac{\nu(\varphi_{c,h}^k)}{\sqrt{\mathrm{trace}(\Pi)}}(\mathbf{u}_{c,h}\cdot\tau_i)(\mathbf{v}_{c,h}\cdot\tau_i)dS,\end{aligned} \tag{3.6}$$

$$b_c(\mathbf{v}_{c,h},q_{c,h})=-(\nabla\cdot\mathbf{v}_{c,h},q_{c,h})_c. \tag{3.7}$$

We also define the buoyancy term $\mathbf{F}^k$ as follows: for $0\le k\le K$,

$$\mathbf{F}^k=\alpha\rho_0 g(\mathrm{T}_h^k-\overline{\mathrm{T}}_h^k)\mathbf{z}. \tag{3.8}$$

In this section, we denote $\nu_j=\nu(\varphi_{j,h}^k,\mathrm{T}_{j,h}^k), j\in\{c,m\}$, $\kappa=\kappa(\mathrm{T}_h^k)$ for simplicity. Then we present the numerical scheme for solving the CHNSDB model (2.8)-(2.21) as follows.

Step 1: find $\varphi_h^{k+1}\in Y_h$ and $\mu_h^{k+1}\in Y_h$ such that for any $v_h,\phi_h\in Y_h$,

$$(\delta_\tau\varphi_h^{k+1},v_h)+(\mathrm{M}(\varphi_h^k)\nabla\mu_h^{k+1},\nabla v_h)-(\overline{\mathbf{u}}_h^{k+1}\varphi_h^k,\nabla v_h)=0, \tag{3.9}$$

$$\gamma\Big[\frac{1}{\epsilon}(f(\varphi_h^{k+1},\varphi_h^k),\phi_h)+\epsilon(\nabla\varphi_h^{k+1},\nabla\phi_h)\Big]-(\mu_h^{k+1},\phi_h)=0. \tag{3.10}$$

Step 2: find $\mathrm{T}_h^{k+1}\in Y_h$ such that for any $W_h\in Y_h$,

$$(\delta_\tau\mathrm{T}_h^{k+1},W_h)+\mathrm{B}(\mathbf{u}_h^k,\mathrm{T}_h^{k+1},W_h)+\left(\kappa(\mathrm{T}_h^k)\nabla\mathrm{T}_h^{k+1},\nabla W_h\right)=0, \tag{3.11}$$

where

$$\mathbf{u}_h^k=\begin{cases}\mathbf{u}_{m,h}^k, & x\in\Omega_m,\\ \mathbf{u}_{c,h}^k, & x\in\Omega_c.\end{cases} \tag{3.12}$$

Step 3: find $\mathbf{u}_{m,h}^{k+1}\in\mathbf{X}_m^h$ and $P_{m,h}^{k+1}\in M_m^h$ such that for any $\mathbf{v}_{m,h}\in\mathbf{X}_m^h$ and $q_{m,h}\in M_m^h$,

$$\left(\frac{\rho_0}{\chi}\delta_\tau\mathbf{u}_{m,h}^{k+1}+\frac{\nu(\varphi_{m,h}^k,\mathrm{T}_{m,h}^k)}{\Pi}\mathbf{u}_{m,h}^{k+1}+\nabla P_{m,h}^{k+1}+\varphi_{m,h}^k\nabla\mu_{m,h}^{k+1},\mathbf{v}_{m,h}\right)_m=\left(\mathbf{F},\mathbf{v}_{m,h}\right)_m. \tag{3.13}$$

$$\beta\tau(\nabla P_{m,h}^{k+1},\nabla q_{m,h})_m-(\mathbf{u}_{m,h}^{k+1},\nabla q_{m,h})_m-\int_{\Gamma_{cm}}\mathbf{u}_{c,h}^k\cdot\mathbf{n}_{cm}q_{m,h}dS=0. \tag{3.14}$$

Step 4: find $\mathbf{u}_{c,h}^{k+1} \in \mathbf{X}_c^h$ and $P_{c,h}^{k+1} \in M_c^h$ such that for any $\mathbf{v}_{c,h} \in \mathbf{X}_c^h$ and $q_{c,h} \in M_c^h$,

$$\begin{aligned}&\rho_0(\delta_\tau \mathbf{u}_{c,h}^{k+1}, \mathbf{v}_{c,h})_c + \rho_0 \mathrm{B}_c(\mathbf{u}_{c,h}^k, \mathbf{u}_{c,h}^{k+1}, \mathbf{v}_{c,h}) + a_c^k(\mathbf{u}_{c,h}^{k+1}, \mathbf{v}_{c,h}) + b_c(\mathbf{v}_{c,h}, P_{c,h}^{k+1}) - b_c(\mathbf{u}_{c,h}^{k+1}, q_{c,h})\\ &+(\varphi_{c,h}^k \nabla \mu_{c,h}^{k+1}, \mathbf{v}_{c,h})_c + \int_{\Gamma_{cm}} P_{m,h}^{k+1}(\mathbf{v}_{c,h} \cdot \mathbf{n}_{cm}) dS = \left(\mathbf{F}, \mathbf{v}_{c,h}\right)_c, \end{aligned} \tag{3.15}$$

where $\mathbf{F}$ is chosen to be $\mathbf{F}^k$ or $\mathbf{F}^{k+1}$. We mention that $\mathbf{F}^k$ allows us to compute heat equation and fluid equations at the same time in each iteration, while the heat equation must be computed before solving the fluid equations with $\mathbf{F}^{k+1}$. The different choices of $\mathbf{F}$ cause a difference in the discrete energy law, which will be presented below. Recall the definition of B_c from (2.44) and that B_c is antisymmetric in the last two variables. We remark that $\mathrm{B}_c(\mathbf{u}_{c,h}^k, \mathbf{u}_{c,h}^{k+1}, \mathbf{v}_{c,h})$ in step 4 is not equal to the original trilinear term $\widetilde{\mathrm{B}}_c(\mathbf{u}_{c,h}^k, \mathbf{u}_{c,h}^{k+1}, \mathbf{v}_{c,h})$ due to the difference between $\mathbf{u}_{c,h}^k$ and $\mathbf{u}_{c,h}^{k+1}$.

3.2 Discrete energy law

To state the energy stability of the fully decoupled scheme mentioned above, we shall define the total discrete energy function as follows:

$$\mathcal{E}_A^k = \int_{\Omega_c} \frac{\rho_0}{2} \left|\mathbf{u}_{c,h}^k\right|^2 dx + \int_{\Omega_m} \frac{\rho_0}{2\chi} \left|\mathbf{u}_{m,h}^k\right|^2 dx + A\int_\Omega \frac{1}{2}(\mathrm{T}_h^k)^2 dx + \gamma \int_\Omega \left[\frac{1}{\epsilon}F(\varphi_h^k) + \frac{\epsilon}{2}|\nabla \varphi_h^k|^2\right] dx, \tag{3.16}$$

where A is the constant that satisfies (2.23). Recalling that $\bar{c}$ is the lower bound of κ, we also define a modified discrete energy

$$\widetilde{\mathcal{E}}_A^k = \int_{\Omega_c} \frac{\rho_0}{2} \left|\mathbf{u}_{c,h}^k\right|^2 dx + \int_{\Omega_m} \frac{\rho_0}{2\chi} \left|\mathbf{u}_{m,h}^k\right|^2 dx + \int_\Omega \left[\frac{A}{2}(\mathrm{T}_h^k)^2 + \frac{\gamma}{\epsilon}F(\varphi_h^k) + \frac{\gamma\epsilon}{2}|\nabla\varphi_h^k|^2\right] dx + A\bar{c}\tau \int_\Omega |\nabla \mathrm{T}_h^k|^2 dx. \tag{3.17}$$

Before we start to prove the discrete energy stability, we recall the following lemma from [9].

Lemma 2 *Suppose $w \in X_m$, and $\mathbf{v}_{c,h} \in \mathbf{X}_c^h$ satisfy*

$$(\nabla \cdot \mathbf{v}_{c,h}, q_{c,h})_c = 0, \quad \forall q_{c,h} \in M_c^h, \tag{3.18}$$

then

$$\left|\int_{\Gamma_{cm}} \mathbf{v}_{c,h} \cdot \mathbf{n}_{cm} w \, dS\right| \le C\|\nabla w\|_{L^2(\Omega_m)} \|\mathbf{v}_{c,h}\|_{L^2(\Omega_c)}. \tag{3.19}$$

We also need several lemmas to estimate the buoyancy terms when dealing with the discrete energy.

Lemma 3 *Suppose* $(\varphi_h^{k+1}, \mu_h^{k+1}, \mathrm{T}_h^{k+1}, \mathbf{u}_{c,h}^{k+1}, P_{c,h}^{k+1}, \mathbf{u}_{m,h}^{k+1}, P_{m,h}^{k+1})$, $0 \le k \le K-1$, *is a solution to the numerical scheme* (3.9)-(3.15) *with* $\mathbf{F} = \mathbf{F}^k$, *and that* A *satisfies* (2.23). *Then for every* $0 \le k \le K-1$ *there holds*

$$\begin{aligned}&\tau\left(\alpha\rho_0 g(\mathrm{T}_{c,h}^k - \overline{\mathrm{T}}_h^k)\mathbf{z}, \mathbf{u}_{c,h}^{k+1}\right)_c + \tau\left(\alpha\rho_0 g(\mathrm{T}_{m,h}^k - \overline{\mathrm{T}}_h^k)\mathbf{z}, \mathbf{u}_{m,h}^{k+1}\right)_m \\ &\le A\bar{c}\tau\left\|\nabla \mathrm{T}_h^k\right\|_{L^2}^2 + \tau a_c^k\left(\mathbf{u}_{c,h}^{k+1}, \mathbf{u}_{c,h}^{k+1}\right) + \tau\left\|\sqrt{\nu_m/\Pi}\mathbf{u}_m^{k+1}\right\|_{L^2}^2. \end{aligned} \tag{3.20}$$

Proof Recall that $\bar{c}$ is the lower bound of κ, λ is the upper bound of the largest eigenvalue of Π, and positive constants C_p, C_k are defined in (2.22). For $\theta = \alpha\rho_0 g$ we have the following estimate

$$\begin{aligned}\theta\left((\mathrm{T}_{c,h}^k - \overline{\mathrm{T}}_h^k)\mathbf{z}, \mathbf{u}_{c,h}^{k+1}\right)_c &\le \theta\left\|\mathrm{T}_{c,h}^k - \overline{\mathrm{T}}_h^k\right\|_{L^2}\left\|\mathbf{u}_c^{k+1}\right\|_{L^2} \le \frac{C_k\theta^2}{8\bar{c}}\left\|\mathrm{T}_{c,h}^k - \overline{\mathrm{T}}_h^k\right\|_{L^2}^2 + \frac{2\bar{c}}{C_k}\left\|\mathbf{u}_c^{k+1}\right\|_{L^2}^2 \\ &\le \frac{A\bar{c}}{C_p}\left\|\mathrm{T}_{c,h}^k - \overline{\mathrm{T}}_h^k\right\|_{L^2}^2 + 2\bar{c}\left\|\mathbb{D}(\mathbf{u}_c^{k+1})\right\|_{L^2}^2. \end{aligned} \tag{3.21}$$

Similarly, we obtain

$$\theta\left((\mathrm{T}_{m,h}^k - \overline{\mathrm{T}}_h^k)\mathbf{z}, \mathbf{u}_{m,h}^{k+1}\right)_m \le \frac{A\bar{c}}{C_p}\left\|\mathrm{T}_{m,h}^k - \overline{\mathrm{T}}_h^k\right\|_{L^2}^2 + \frac{\bar{c}}{\lambda}\left\|\mathbf{u}_m^{k+1}\right\|_{L^2}^2. \tag{3.22}$$

It follows that

$$\begin{aligned}&\theta\left((\mathrm{T}_{c,h}^k - \overline{\mathrm{T}}_h^k)\mathbf{z}, \mathbf{u}_{c,h}^{k+1}\right)_c + \theta\left((\mathrm{T}_{m,h}^k - \overline{\mathrm{T}}_h^k)\mathbf{z}, \mathbf{u}_{m,h}^{k+1}\right)_m \\ &\le \frac{A\bar{c}}{C_p}\left\|\mathrm{T}_h^k - \overline{\mathrm{T}}_h^k\right\|_{L^2}^2 + 2\bar{c}\left\|\mathbb{D}(\mathbf{u}_c^{k+1})\right\|_{L^2}^2 + \frac{\bar{c}}{\lambda}\left\|\mathbf{u}_m^{k+1}\right\|_{L^2}^2 \\ &\le A\bar{c}\left\|\nabla \mathrm{T}_h^k\right\|_{L^2}^2 + a_c^k\left(\mathbf{u}_{c,h}^{k+1}, \mathbf{u}_{c,h}^{k+1}\right) + \left\|\sqrt{\nu_m/\Pi}\mathbf{u}_m^{k+1}\right\|_{L^2}^2. \end{aligned} \tag{3.23}$$

Multiplying the inequality by τ, we derive

$$\begin{aligned}&\tau\left(\alpha\rho_0 g(\mathrm{T}_{c,h}^k - \overline{\mathrm{T}}_h^k)\mathbf{z}, \mathbf{u}_{c,h}^{k+1}\right)_c + \tau\left(\alpha\rho_0 g(\mathrm{T}_{m,h}^k - \overline{\mathrm{T}}_h^k)\mathbf{z}, \mathbf{u}_{m,h}^{k+1}\right)_m \\ &\le A\bar{c}\tau\left\|\nabla \mathrm{T}_h^k\right\|_{L^2}^2 + \tau a_c^k\left(\mathbf{u}_{c,h}^{k+1}, \mathbf{u}_{c,h}^{k+1}\right) + \tau\left\|\sqrt{\nu_m/\Pi}\mathbf{u}_m^{k+1}\right\|_{L^2}^2. \end{aligned} \tag{3.24}$$

This concludes the proof of the lemma. □

Similarly, we have the following lemma.

Lemma 4 *Suppose* $(\varphi_h^{k+1}, \mu_h^{k+1}, \mathrm{T}_h^{k+1}, \mathbf{u}_{c,h}^{k+1}, P_{c,h}^{k+1}, \mathbf{u}_{m,h}^{k+1}, P_{m,h}^{k+1})$, $0 \le k \le K-1$, *is a solution to the numerical scheme* (3.9)-(3.15) *with* $\mathbf{F} = \mathbf{F}^{k+1}$. *Recall* $\bar{c}$ *the lower bound of* κ. *Then for every* $0 \le k \le K-1$ *there holds*

$$\begin{aligned}&\tau\left(\alpha\rho_0 g(\mathrm{T}_{c,h}^{k+1} - \overline{\mathrm{T}}_h^{k+1})\mathbf{z}, \mathbf{u}_{c,h}^{k+1}\right)_c + \tau\left(\alpha\rho_0 g(\mathrm{T}_{m,h}^{k+1} - \overline{\mathrm{T}}_h^{k+1})\mathbf{z}, \mathbf{u}_{m,h}^{k+1}\right)_m \\ &\le A\bar{c}\tau\left\|\nabla \mathrm{T}_h^{k+1}\right\|_{L^2}^2 + \tau a_c^k\left(\mathbf{u}_{c,h}^{k+1}, \mathbf{u}_{c,h}^{k+1}\right) + \tau\left\|\sqrt{\nu_m/\Pi}\mathbf{u}_m^{k+1}\right\|_{L^2}^2. \end{aligned} \tag{3.25}$$

Now we are able to demonstrate the uniquely solvability and energy stability of the scheme by the following theorem.

Theorem 1 *The numerical scheme* (3.9)-(3.15) *with* $\mathbf{F} = \mathbf{F}^k$ *is unconditionally uniquely solvable at each time step, and it satisfies the following energy law that for all* $0 \leq k \leq K-1$,

$$\begin{aligned}
&\widetilde{\mathcal{E}}_A^{k+1} - \widetilde{\mathcal{E}}_A^k + \tau||\sqrt{\mathrm{M}}\nabla\mu_h^{k+1}||_{L^2}^2 + \frac{\beta\tau^2}{2}||\nabla P_{m,h}^{k+1}||_{L^2}^2 + \frac{\tau^2}{4\rho_0}\left(\chi\|\varphi_{m,h}^k\nabla\mu_{m,h}^{k+1}\|^2 + \|\varphi_{c,h}^k\nabla\mu_{c,h}^{k+1}\|^2\right) \\
&\leq -\frac{\gamma\epsilon}{2}||\nabla(\varphi_h^{k+1}-\varphi_h^k)||_{L^2}^2 - \frac{\rho_0}{12}\|\mathbf{u}_{c,h}^{k+1}-\mathbf{u}_{c,h}^k\|_{L^2}^2 - \frac{\rho_0}{6\chi}\|\mathbf{u}_{m,h}^{k+1}-\mathbf{u}_{m,h}^k\|_{L^2}^2 - \frac{A}{2}\|\mathrm{T}_h^{k+1}-\mathrm{T}_h^k\|_{L^2}^2, \qquad (3.26)
\end{aligned}$$

where $\mathrm{M} = \mathrm{M}(\varphi_h^k)$, *and* A *is a constant satisfying* (2.23).

Proof First, we show the unique solvability. Note that the non-linear Cahn-Hilliard equations (3.9)-(3.10) are completely decoupled from heat equation (3.11), Darcy equations (3.13)-(3.14) and Navier-Stokes equation (3.15). In detail, the intermediate velocity function $\overline{\mathbf{u}}_h^{k+1}$ is determined by $\mathbf{u}_h^k$, φ_h^k calculated at the former time step and the unknown μ_h^{k+1}, then the third term in (3.9) is a linear term with respect to $\nabla\mu_h^{k+1}$ just as the second term. Thus, given $\mathbf{u}_h^k, \varphi_h^k$, (3.9)-(3.10) can be viewed as a first-order convex-splitting discretization of the Cahn-Hilliard equation with known source terms, and the unique solvability of the Cahn-Hilliard system can be explained with a gradient flow argument [31] [35] [44]. With μ_h^{k+1} obtained, (3.11)-(3.15) define a finite linear system for $\mathrm{T}_h^{k+1}, \mathbf{u}_{m,h}^{k+1}, P_{m,h}^{k+1}, \mathbf{u}_{c,h}^{k+1}, P_{c,h}^{k+1}$. Thus we only need to show that the solutions are unique. Suppose there are two solutions to (3.11)-(3.15). Denote $e_T, \mathbf{e}_c^u, e_c^p, \mathbf{e}_m^u, e_m^p$ the differences between two solutions respectively. Then the following estimate holds for any $W_h \in Y_h$,

$$(\frac{e_T}{\tau}, W_h) + \mathrm{B}(\mathbf{u}_h^k, e_T, W_h) + \left(\kappa(T_h^k)\nabla e_T, \nabla W_h\right) = 0. \qquad (3.27)$$

Take $W_h = e_T$ and recall the definition (2.41) for $\mathrm{B}(\mathbf{u}, v, w)$, one gets

$$(\frac{e_T}{\tau}, e_T) + \left(\kappa(T_h^k)\nabla e_T, \nabla e_T\right) = 0, \qquad (3.28)$$

and so $e_T = 0$. Thus T_h^{k+1} is uniquely determined and so are the viscosity coefficients ν_c, ν_m in the fluid system at the same time step. Next, for all $\mathbf{v}_{c,h} \in \mathbf{X}_c^h$, $q_{c,h} \in M_c^h$, $\mathbf{v}_{m,h} \in \mathbf{X}_m^h$, $q_{m,h} \in M_m^h$, we have

$$\left(\frac{\rho_0}{\chi\tau}\mathbf{e}_m^u + \frac{\nu_m}{\Pi}\mathbf{e}_m^u + \nabla e_m^p, \mathbf{v}_{m,h}\right)_m = 0, \qquad (3.29)$$

$$\beta\tau\left(\nabla e_m^p, \nabla q_{m,h}\right)_m - \left(\mathbf{e}_m^u, \nabla q_{m,h}\right)_m = 0, \qquad (3.30)$$

$$\frac{\rho_0}{\tau}(\mathbf{e}_c^u, \mathbf{v}_{c,h})_c + \rho_0\mathrm{B}_c(\mathbf{u}_{c,h}^k, \mathbf{e}_c^u, \mathbf{v}_{c,h}) + a_c^k(\mathbf{e}_c^u, \mathbf{v}_{c,h}) + b_c(\mathbf{v}_{c,h}, e_c^p)$$

$$+\int_{\Gamma_{cm}} e_m^p(\mathbf{v}_{c,h}\cdot\mathbf{n}_{cm})dS - b_c(\mathbf{e}_c^u, q_{c,h}) = 0. \tag{3.31}$$

Set $\mathbf{v}_{m,h} = \mathbf{e}_m^u,\ q_{m,h} = e_m^p$, adding (3.29) and (3.30) together, and by the fact that $e_m^p \in M_m^h$ where the mean value on Ω_m is zero, we obtain $\mathbf{e}_m^u = 0,\ e_m^p = 0$. Similarly, set $\mathbf{v}_{c,h} = \mathbf{e}_c^u,\ q_{c,h} = e_c^p$. Thanks to the definition of $\mathrm{B}_c(\mathbf{u},\mathbf{v},\mathbf{w})$, we have $\mathrm{B}_c(\mathbf{u}_{c,h}^k, \mathbf{e}_c^u, \mathbf{e}_c^u) = 0$, and then, applying $e_m^p = 0$, (3.31) is equivalent to

$$\frac{\rho_0}{\tau}(\mathbf{e}_c^u, \mathbf{e}_c^u)_c + a_c^k(\mathbf{e}_c^u, \mathbf{e}_c^u) = 0, \tag{3.32}$$

hence $\mathbf{e}_c^u = 0$. Now (3.31) can be derived as $b_c(\mathbf{v}_{c,h}, e_c^p) = 0$, which holds for all $\mathbf{v}_{c,h} \in \mathbf{X}_c^h$. By inf-sup condition (3.1) one obtains $e_c^p = 0$. This ends the proof of unique solvability.

Then we prove the discrete energy law (3.26). Take $v_h = \tau\mu_h^{k+1}$ in (3.9), $\phi_h = \varphi_h^{k+1} - \varphi_h^k$ in (3.10), adding them together and thanks to the following estimate due to the convexity

$$F(\varphi_h^{k+1}) - F(\varphi_h^k) \le f(\varphi_h^{k+1}, \varphi_h^k)(\varphi_h^{k+1} - \varphi_h^k), \tag{3.33}$$

one obtains

$$E(\varphi_h^{k+1}) - E(\varphi_h^k) + \tau\|\sqrt{\mathrm{M}}\nabla\mu_h^{k+1}\|_{L^2}^2 + \frac{\gamma\epsilon}{2}\|\nabla(\varphi_h^{k+1} - \varphi_h^k)\|_{L^2}^2 \le \tau(\overline{\mathbf{u}}_h^{k+1}\varphi_h^k, \nabla\mu_h^{k+1}). \tag{3.34}$$

By (3.4) and (3.5), we can rewrite (3.34) as follows

$$\begin{aligned} &E(\varphi_h^{k+1}) - E(\varphi_h^k) + \tau\|\sqrt{\mathrm{M}}\nabla\mu_h^{k+1}\|_{L^2}^2 + \frac{\gamma\epsilon}{2}\|\nabla(\varphi_h^{k+1} - \varphi_h^k)\|_{L^2}^2 \\ &+\frac{\tau^2}{\rho_0}\left(\chi\|\varphi_{m,h}^k\nabla\mu_{m,h}^{k+1}\|^2 + \|\varphi_{c,h}^k\nabla\mu_{c,h}^{k+1}\|^2\right) \ \le\ \tau(\mathbf{u}_h^k\varphi_h^k, \nabla\mu_h^{k+1}). \end{aligned} \tag{3.35}$$

Taking $W_h = A\tau\mathrm{T}_h^{k+1}$ in (3.11), we get

$$\frac{A}{2}\{\|\mathrm{T}_h^{k+1}\|_{L^2}^2 - \|\mathrm{T}_h^k\|_{L^2}^2 + \|\mathrm{T}_h^{k+1} - \mathrm{T}_h^k\|_{L^2}^2\} + A\tau\|\sqrt{\kappa}\nabla\mathrm{T}_h^{k+1}\|_{L^2}^2 = 0. \tag{3.36}$$

Letting $\mathbf{v}_{c,h} = \tau\mathbf{u}_{c,h}^{k+1}$ and $q_{c,h} = \tau P_{c,h}^{k+1}$ in (3.15), using the antisymmetric quality of $\mathrm{B}_c(\mathbf{u},\mathbf{v},\mathbf{w})$ with respect to the variables $\mathbf{v}$ and $\mathbf{w}$, one has

$$\begin{aligned} &\frac{\rho_0}{2}\{||\mathbf{u}_{c,h}^{k+1}||_{L^2}^2 - ||\mathbf{u}_{c,h}^k||_{L^2}^2 + ||\mathbf{u}_{c,h}^{k+1} - \mathbf{u}_{c,h}^k||_{L^2}^2\} + \tau a_c^k(\mathbf{u}_{c,h}^{k+1}, \mathbf{u}_{c,h}^{k+1}) \\ &+\tau\int_{\Gamma_{cm}} P_{m,h}^{k+1}(\mathbf{u}_{c,h}^{k+1}\cdot\mathbf{n}_{cm})dS + \tau(\mathbf{u}_{c,h}^{k+1}\varphi_{c,h}^k, \nabla\mu_{c,h}^{k+1})_c = \tau\left(\alpha\rho_0 g(\mathrm{T}_{c,h}^k - \overline{\mathrm{T}}_h^k)\mathbf{z}, \mathbf{u}_{c,h}^{k+1}\right)_c. \end{aligned} \tag{3.37}$$

Similarly, set $\mathbf{v}_{m,h} = \tau\mathbf{u}_{m,h}^{k+1}$ in (3.13) and $q_{m,h} = \tau P_{m,h}^{k+1}$ in (3.14), summing up the results and we derive

$$\frac{\rho_0}{2\chi}\{||\mathbf{u}_{m,h}^{k+1}||_{L^2}^2 - ||\mathbf{u}_{m,h}^k||_{L^2}^2 + ||\mathbf{u}_{m,h}^{k+1} - \mathbf{u}_{m,h}^k||_{L^2}^2\} + \tau\left\|\sqrt{\nu_m/\Pi}\mathbf{u}_{m,h}^{k+1}\right\|_{L^2}^2 + \beta\tau^2||\nabla P_{m,h}^{k+1}||_{L^2}^2$$

$$+\tau(\mathbf{u}_{m,h}^{k+1}\varphi_{m,h}^{k},\nabla\mu_{m,h}^{k+1})_m-\tau\int_{\Gamma_{cm}}\mathbf{u}_{c,h}^{k}\cdot\mathbf{n}_{cm}P_{m,h}^{k+1}\,dS=\tau\left(\alpha\rho_0 g(\mathrm{T}_{m,h}^{k}-\overline{\mathrm{T}}_h^{k})\mathbf{z},\mathbf{u}_{m,h}^{k+1}\right)_m. \tag{3.38}$$

By summing up the above estimates (3.35), (3.36), (3.37) and (3.38), we obtain

$$\begin{aligned}
&\mathcal{E}_A^{k+1}-\mathcal{E}_A^{k}+\tau||\sqrt{\mathrm{M}}\nabla\mu_h^{k+1}||_{L^2}^2+\tau a_c^k(\mathbf{u}_{c,h}^{k+1},\mathbf{u}_{c,h}^{k+1})+\tau\big\|\sqrt{\nu_m/\Pi}\mathbf{u}_{m,h}^{k+1}\big\|_{L^2}^2+A\tau\|\sqrt{\kappa}\nabla\mathrm{T}_h^{k+1}\|_{L^2}^2\\
&+\beta\tau^2||\nabla P_{m,h}^{k+1}||_{L^2}^2+\frac{\tau^2}{\rho_0}\left(\chi\|\varphi_{m,h}^{k}\nabla\mu_{m,h}^{k+1}\|^2+\|\varphi_{c,h}^{k}\nabla\mu_{c,h}^{k+1}\|^2\right)+\frac{A}{2}\|\mathrm{T}_h^{k+1}-\mathrm{T}_h^{k}\|_{L^2}^2\\
&+\frac{\gamma\epsilon}{2}||\nabla(\varphi_h^{k+1}-\varphi_h^{k})||_{L^2}^2+\frac{\rho_0}{2}\|\mathbf{u}_{c,h}^{k+1}-\mathbf{u}_{c,h}^{k}\|_{L^2}^2+\frac{\rho_0}{2\chi}\|\mathbf{u}_{m,h}^{k+1}-\mathbf{u}_{m,h}^{k}\|_{L^2}^2\\
\le&-\tau(\mathbf{u}_h^{k+1}-\mathbf{u}_h^{k},\varphi_h^{k}\nabla\mu_h^{k+1})\;-\tau\int_{\Gamma_{cm}}(\mathbf{u}_{c,h}^{k+1}-\mathbf{u}_{c,h}^{k})\cdot\mathbf{n}_{cm}P_{m,h}^{k+1}dS\\
&+\tau\left(\alpha\rho_0 g(\mathrm{T}_{c,h}^{k}-\overline{\mathrm{T}}_h^{k})\mathbf{z},\mathbf{u}_{c,h}^{k+1}\right)_c+\tau\left(\alpha\rho_0 g(\mathrm{T}_{m,h}^{k}-\overline{\mathrm{T}}_h^{k})\mathbf{z},\mathbf{u}_{m,h}^{k+1}\right)_m.
\end{aligned}\tag{3.39}$$

By the inequality $(a,b)\le\frac{a^2}{3}+\frac{3b^2}{4}$, we have

$$\begin{aligned}
-\tau(\mathbf{u}_h^{k+1}-\mathbf{u}_h^{k},\varphi_h^{k}\nabla\mu_h^{k+1})\le&\frac{\rho_0}{3}||\mathbf{u}_{c,h}^{k+1}-\mathbf{u}_{c,h}^{k}||_{L^2}^2+\frac{\rho_0}{3\chi}||\mathbf{u}_{m,h}^{k+1}-\mathbf{u}_{m,h}^{k}||_{L^2}^2\\
&+\frac{3\tau^2}{4\rho_0}\left(\chi\|\varphi_{m,h}^{k}\nabla\mu_{m,h}^{k+1}\|^2+\|\varphi_{c,h}^{k}\nabla\mu_{c,h}^{k+1}\|^2\right).
\end{aligned}\tag{3.40}$$

Using Lemma 2, we have the following estimate

$$\begin{aligned}
-\tau\int_{\Gamma_{cm}}(\mathbf{u}_{c,h}^{k+1}-\mathbf{u}_{c,h}^{k})\cdot\mathbf{n}_{cm}P_{m,h}^{k+1}dS\le&C\tau\|\mathbf{u}_{c,h}^{k+1}-\mathbf{u}_{c,h}^{k}\|_{L^2}\|\nabla P_{m,h}^{k+1}\|_{L^2}\\
\le&\frac{\rho_0}{12}\|\mathbf{u}_{c,h}^{k+1}-\mathbf{u}_{c,h}^{k}\|_{L^2}^2+C_1\tau^2\|\nabla P_{m,h}^{k+1}\|_{L^2},
\end{aligned}\tag{3.41}$$

where C_1 depends only on Ω_m, Ω_c and ρ_0. Adding (3.39), (3.40) and (3.41) together we obtain

$$\begin{aligned}
&\mathcal{E}_A^{k+1}-\mathcal{E}_A^{k}+\tau||\sqrt{\mathrm{M}}\nabla\mu_h^{k+1}||_{L^2}^2+\tau a_c^k(\mathbf{u}_{c,h}^{k+1},\mathbf{u}_{c,h}^{k+1})+\tau\big\|\sqrt{\nu_m/\Pi}\mathbf{u}_{m,h}^{k+1}\big\|_{L^2}^2+A\tau\|\sqrt{\kappa}\nabla\mathrm{T}_h^{k+1}\|_{L^2}^2\\
&+\frac{\beta\tau^2}{2}||\nabla P_{m,h}^{k+1}||_{L^2}^2+\frac{\tau^2}{4\rho_0}\left(\chi\|\varphi_{m,h}^{k}\nabla\mu_{m,h}^{k+1}\|^2+\|\varphi_{c,h}^{k}\nabla\mu_{c,h}^{k+1}\|^2\right)+\frac{A}{2}\|\mathrm{T}_h^{k+1}-\mathrm{T}_h^{k}\|_{L^2}^2\\
&+\frac{\gamma\epsilon}{2}||\nabla(\varphi_h^{k+1}-\varphi_h^{k})||_{L^2}^2+\frac{\rho_0}{12}\|\mathbf{u}_{c,h}^{k+1}-\mathbf{u}_{c,h}^{k}\|_{L^2}^2+\frac{\rho_0}{6\chi}\|\mathbf{u}_{m,h}^{k+1}-\mathbf{u}_{m,h}^{k}\|_{L^2}^2\\
\le&\tau\left(\alpha\rho_0 g(\mathrm{T}_{c,h}^{k}-\overline{\mathrm{T}}_h^{k})\mathbf{z},\mathbf{u}_{c,h}^{k+1}\right)_c+\tau\left(\alpha\rho_0 g(\mathrm{T}_{m,h}^{k}-\overline{\mathrm{T}}_h^{k})\mathbf{z},\mathbf{u}_{m,h}^{k+1}\right)_m,
\end{aligned}\tag{3.42}$$

where $\beta\ge 2C_1$. Now we use the estimate in Lemma 3 for the right-hand-side(RHS) term of (3.42), and we obtain

$$\begin{aligned}
&\mathcal{E}_A^{k+1}-\mathcal{E}_A^{k}+\tau||\sqrt{\mathrm{M}}\nabla\mu_h^{k+1}||_{L^2}^2+\tau a_c^k(\mathbf{u}_{c,h}^{k+1},\mathbf{u}_{c,h}^{k+1})+\tau\big\|\sqrt{\nu_m/\Pi}\mathbf{u}_{m,h}^{k+1}\big\|_{L^2}^2+A\tau\|\sqrt{\kappa}\nabla\mathrm{T}_h^{k+1}\|_{L^2}^2\\
&+\frac{\beta\tau^2}{2}||\nabla P_{m,h}^{k+1}||_{L^2}^2+\frac{\tau^2}{4\rho_0}\left(\chi\|\varphi_{m,h}^{k}\nabla\mu_{m,h}^{k+1}\|^2+\|\varphi_{c,h}^{k}\nabla\mu_{c,h}^{k+1}\|^2\right)+\frac{A}{2}\|\mathrm{T}_h^{k+1}-\mathrm{T}_h^{k}\|_{L^2}^2\\
&+\frac{\gamma\epsilon}{2}||\nabla(\varphi_h^{k+1}-\varphi_h^{k})||_{L^2}^2+\frac{\rho_0}{12}\|\mathbf{u}_{c,h}^{k+1}-\mathbf{u}_{c,h}^{k}\|_{L^2}^2+\frac{\rho_0}{6\chi}\|\mathbf{u}_{m,h}^{k+1}-\mathbf{u}_{m,h}^{k}\|_{L^2}^2
\end{aligned}$$

$$\leq A\bar{c}\tau \left\|\nabla \mathrm{T}_h^k\right\|_{L^2}^2 + \tau a_c^k\left(\mathbf{u}_{c,h}^{k+1}, \mathbf{u}_{c,h}^{k+1}\right) + \tau \left\|\sqrt{\nu_m/\Pi}\mathbf{u}_m^{k+1}\right\|_{L^2}^2. \tag{3.43}$$

Notice that

$$\widetilde{\mathcal{E}}_A^{k+1} = \mathcal{E}_A^{k+1} + A\bar{c}\tau \left\|\nabla \mathrm{T}_h^{k+1}\right\|_{L^2}^2 \leq \mathcal{E}_A^{k+1} + A\tau \left\|\sqrt{\kappa}\nabla \mathrm{T}_h^{k+1}\right\|_{L^2}^2,$$
$$\widetilde{\mathcal{E}}_A^{k} = \mathcal{E}_A^{k} + A\bar{c}\tau \left\|\nabla \mathrm{T}_h^{k}\right\|_{L^2}^2,$$

then we obtain the following modified discrete energy law

$$\begin{aligned}
&\widetilde{\mathcal{E}}_A^{k+1} - \widetilde{\mathcal{E}}_A^{k} + \tau||\sqrt{\mathrm{M}}\nabla\mu_h^{k+1}||_{L^2}^2 + \frac{\beta\tau^2}{2}||\nabla P_{m,h}^{k+1}||_{L^2}^2 + \frac{\tau^2}{4\rho_0}\left(\chi\|\varphi_{m,h}^k\nabla\mu_{m,h}^{k+1}\|^2 + \|\varphi_{c,h}^k\nabla\mu_{c,h}^{k+1}\|^2\right)\\
\leq& -\frac{\gamma\epsilon}{2}||\nabla(\varphi_h^{k+1} - \varphi_h^k)||_{L^2}^2 - \frac{\rho_0}{12}\|\mathbf{u}_{c,h}^{k+1} - \mathbf{u}_{c,h}^k\|_{L^2}^2 - \frac{\rho_0}{6\chi}\|\mathbf{u}_{m,h}^{k+1} - \mathbf{u}_{m,h}^k\|_{L^2}^2 - \frac{A}{2}\|\mathrm{T}_h^{k+1} - \mathrm{T}_h^k\|_{L^2}^2.
\end{aligned} \tag{3.44}$$

This completes the proof. □

Theorem 2 *The numerical scheme* (3.9)-(3.15) *with* $\mathbf{F} = \mathbf{F}^{k+1}$ *is unconditionally uniquely solvable at each time step, and it satisfies the following energy laws that for all* $0 \leq k \leq K-1$,

$$\begin{aligned}
&\mathcal{E}_A^{k+1} - \mathcal{E}_A^{k} + \tau||\sqrt{\mathrm{M}}\nabla\mu_h^{k+1}||_{L^2}^2 + \frac{\beta\tau^2}{2}||\nabla P_{m,h}^{k+1}||_{L^2}^2 + \frac{\tau^2}{4\rho_0}\left(\chi\|\varphi_{m,h}^k\nabla\mu_{m,h}^{k+1}\|^2 + \|\varphi_{c,h}^k\nabla\mu_{c,h}^{k+1}\|^2\right)\\
&+\frac{A}{2}\|\mathrm{T}_h^{k+1} - \mathrm{T}_h^k\|_{L^2}^2 + \frac{\gamma\epsilon}{2}||\nabla(\varphi_h^{k+1} - \varphi_h^k)||_{L^2}^2 + \frac{\rho_0}{12}\|\mathbf{u}_{c,h}^{k+1} - \mathbf{u}_{c,h}^k\|_{L^2}^2 + \frac{\rho_0}{6\chi}\|\mathbf{u}_{m,h}^{k+1} - \mathbf{u}_{m,h}^k\|_{L^2}^2 \leq 0,
\end{aligned} \tag{3.45}$$

where $\mathrm{M} = \mathrm{M}(\varphi_h^k)$, *and* A *is the constant satisfying* (2.23).

Proof The unique solvability is the same as Theorem 1. Additionally, the RHS term in (3.42) is changed here while the left-hand side remains unchanged, that is

$$\begin{aligned}
&\mathcal{E}_A^{k+1} - \mathcal{E}_A^{k} + \tau||\sqrt{\mathrm{M}}\nabla\mu_h^{k+1}||_{L^2}^2 + \tau a_c^k(\mathbf{u}_{c,h}^{k+1}, \mathbf{u}_{c,h}^{k+1}) + \tau\left\|\sqrt{\nu_m/\Pi}\mathbf{u}_{m,h}^{k+1}\right\|_{L^2}^2 + A\tau\|\sqrt{\kappa}\nabla\mathrm{T}_h^{k+1}\|_{L^2}^2\\
&+\frac{\beta\tau^2}{2}||\nabla P_{m,h}^{k+1}||_{L^2}^2 + \frac{\tau^2}{4\rho_0}\left(\chi\|\varphi_{m,h}^k\nabla\mu_{m,h}^{k+1}\|^2 + \|\varphi_{c,h}^k\nabla\mu_{c,h}^{k+1}\|^2\right) + \frac{A}{2}\|\mathrm{T}_h^{k+1} - \mathrm{T}_h^k\|_{L^2}^2\\
&+\frac{\gamma\epsilon}{2}||\nabla(\varphi_h^{k+1} - \varphi_h^k)||_{L^2}^2 + \frac{\rho_0}{12}\|\mathbf{u}_{c,h}^{k+1} - \mathbf{u}_{c,h}^k\|_{L^2}^2 + \frac{\rho_0}{6\chi}\|\mathbf{u}_{m,h}^{k+1} - \mathbf{u}_{m,h}^k\|_{L^2}^2\\
&\leq \tau\left(\alpha\rho_0 g(\mathrm{T}_{c,h}^{k+1} - \overline{\mathrm{T}}_h^{k+1})\mathbf{z}, \mathbf{u}_{c,h}^{k+1}\right)_c + \tau\left(\alpha\rho_0 g(\mathrm{T}_{m,h}^{k+1} - \overline{\mathrm{T}}_h^{k+1})\mathbf{z}, \mathbf{u}_{m,h}^{k+1}\right)_m,
\end{aligned} \tag{3.46}$$

with $\beta \geq 2C_1$ and C_1 is the positive constant in (3.41). Now applying the estimate in Lemma 4 to (3.46), we derive

$$\begin{aligned}
&\mathcal{E}_A^{k+1} - \mathcal{E}_A^{k} + \tau||\sqrt{\mathrm{M}}\nabla\mu_h^{k+1}||_{L^2}^2 + \tau a_c^k(\mathbf{u}_{c,h}^{k+1}, \mathbf{u}_{c,h}^{k+1}) + \tau\left\|\sqrt{\nu_m/\Pi}\mathbf{u}_{m,h}^{k+1}\right\|_{L^2}^2 + A\tau\|\sqrt{\kappa}\nabla\mathrm{T}_h^{k+1}\|_{L^2}^2\\
&+\frac{\beta\tau^2}{2}||\nabla P_{m,h}^{k+1}||_{L^2}^2 + \frac{\tau^2}{4\rho_0}\left(\chi\|\varphi_{m,h}^k\nabla\mu_{m,h}^{k+1}\|^2 + \|\varphi_{c,h}^k\nabla\mu_{c,h}^{k+1}\|^2\right) + \frac{A}{2}\|\mathrm{T}_h^{k+1} - \mathrm{T}_h^k\|_{L^2}^2
\end{aligned}$$

$$
\begin{aligned}
&+\frac{\gamma\epsilon}{2}||\nabla(\varphi_h^{k+1}-\varphi_h^k)||_{L^2}^2+\frac{\rho_0}{12}\|\mathbf{u}_{c,h}^{k+1}-\mathbf{u}_{c,h}^k\|_{L^2}^2+\frac{\rho_0}{6\chi}\|\mathbf{u}_{m,h}^{k+1}-\mathbf{u}_{m,h}^k\|_{L^2}^2\\
&\leq A\bar{c}\tau\left\|\nabla \mathrm{T}_h^{k+1}\right\|_{L^2}^2+\tau a_c^k\left(\mathbf{u}_{c,h}^{k+1},\mathbf{u}_{c,h}^{k+1}\right)+\tau\left\|\sqrt{\nu_m/\Pi}\mathbf{u}_m^{k+1}\right\|_{L^2}^2\\
&\leq A\tau\left\|\sqrt{\kappa}\nabla \mathrm{T}_h^{k+1}\right\|_{L^2}^2+\tau a_c^k\left(\mathbf{u}_{c,h}^{k+1},\mathbf{u}_{c,h}^{k+1}\right)+\tau\left\|\sqrt{\nu_m/\Pi}\mathbf{u}_m^{k+1}\right\|_{L^2}^2,
\end{aligned}
\tag{3.47}
$$

thus the following estimate holds

$$
\begin{aligned}
&\mathcal{E}_A^{k+1}-\mathcal{E}_A^k+\tau||\sqrt{\mathrm{M}}\nabla\mu_h^{k+1}||_{L^2}^2+\frac{\beta\tau^2}{2}||\nabla P_{m,h}^{k+1}||_{L^2}^2+\frac{\tau^2}{4\rho_0}\left(\chi\|\varphi_{m,h}^k\nabla\mu_{m,h}^{k+1}\|^2+\|\varphi_{c,h}^k\nabla\mu_{c,h}^{k+1}\|^2\right)\\
&+\frac{A}{2}\|\mathrm{T}_h^{k+1}-\mathrm{T}_h^k\|_{L^2}^2+\frac{\gamma\epsilon}{2}||\nabla(\varphi_h^{k+1}-\varphi_h^k)||_{L^2}^2+\frac{\rho_0}{12}\|\mathbf{u}_{c,h}^{k+1}-\mathbf{u}_{c,h}^k\|_{L^2}^2+\frac{\rho_0}{6\chi}\|\mathbf{u}_{m,h}^{k+1}-\mathbf{u}_{m,h}^k\|_{L^2}^2\leq 0.
\end{aligned}
\tag{3.48}
$$

This completes the proof. □

4 Numerical experiments

In this section, we present some numerical examples to show that our scheme is accurate for the simulation of two-phase flow with thermal conduction. In the first subsection, we use different examples to numerically demonstrate that our scheme is of first order accuracy in time. The second subsection indicates that the scheme is long-time stable. In the last subsection, we show that our model illustrates well in the sense of convection cells (also called Bénard Cells [1]) where the temperature at top is lower than that at bottom. All the numerical experiments are operated using the software FreeFem++[29].

4.1 Convergence

Now we consider the convergence results of the numerical scheme. In the experiment we set the dimension of the PDE system $d = 2$. Set $\Omega_m = [0,1]\times[0,1]$, $\Omega_c = [0,1]\times[-1,0]$, $\Omega = \Omega_m \cup \Omega_c = [0,1]\times[-1,1]$, $\Gamma_{cm} = [0,1]\times\{0\}$. The value of parameters in the PDE system are showed in Table 1. Note that for simplicity, $\nu(\varphi, \mathrm{T})$ is set to be constant in the convergence test.

PDE parameters	κ	ρ_0	χ	ν_c	ν_m	Π	M(Mobility)	γ	ϵ	α_{BJSJ}	β	α	g
Value in test	0.001	1	1	0.1	0.1	$0.1\mathbb{I}_2$	0.1	0.1	0.1	$\sqrt{0.1}$	1	0.01	10

Table 1: PDE parameters in convergence experiment. $\mathbb{I}_2$ represents the two-dimensional unit matrix.

Here we build the exact solution as follows: for $t \in [0, \mathcal{T}]$,

$$\varphi = e^{-t}\cos(\pi x)\cos(\pi y), \quad (x,y) \in \Omega, \tag{4.1}$$

$$\mathrm{T} = 2 + e^{-t}\cos(\pi x)\cos(\pi y), \quad (x,y) \in \Omega, \tag{4.2}$$

$$\begin{cases} \mathbf{u}_j = e^{-t}\begin{pmatrix} -\frac{1}{2}\sin^2(\pi x)\sin(\pi(y+1)) \\ \sin(2\pi x)\sin^2(\frac{\pi(y+1)}{2}) \end{pmatrix}, & (x,y) \in \Omega_j, \\ & j \in \{c, m\}. \\ P_j = \dfrac{1}{\pi}e^{-t}\sin^2(\pi x)\sin^2(\pi y), & (x,y) \in \Omega_j, \end{cases} \tag{4.3}$$

It satisfies the following PDE system with the right hand side terms f_1, f_2, f_3, f_4,

$$\rho_0(\partial_t \mathbf{u}_c + (\mathbf{u}_c \cdot \nabla)\mathbf{u}_c) - \nabla \cdot \mathbb{T}(\mathbf{u}_c, P_c) + \varphi_c \nabla \mu_c - \alpha\rho_0 g(\mathrm{T}_c - \overline{\mathrm{T}})\mathbf{z} = f_1, \quad \text{in } \Omega_c, \tag{4.4}$$

$$\frac{\rho_0}{\chi}\partial_t \mathbf{u}_m + \nu(\varphi_m)\Pi^{-1}\mathbf{u}_m + \nabla P_m + \varphi_m \nabla \mu_m - \alpha\rho_0 g(\mathrm{T}_m - \overline{\mathrm{T}})\mathbf{z} = f_2, \quad \text{in } \Omega_m, \tag{4.5}$$

$$\nabla \cdot \mathbf{u}_j = 0, \quad \text{in } \Omega_j, \tag{4.6}$$

$$\partial_t \mathrm{T}_j + \mathbf{u}_j \cdot \nabla \mathrm{T}_j - \kappa_j \Delta \mathrm{T}_j = f_3, \quad \text{in } \Omega_j, \tag{4.7}$$

$$\partial_t \varphi_j + \nabla \cdot (\mathbf{u}_j \varphi_j) - \mathrm{div}(\mathrm{M}(\varphi_j)\nabla \mu_j) = f_4, \quad \text{in } \Omega_j, \tag{4.8}$$

where f_1, f_2, f_3, f_4 can be determined by (4.1)-(4.3).The exact solution above satisfies the same boundary and interface conditions as (2.8)-(2.13), except for the last two interface conditions (2.14)-(2.15). Here these two interface conditions will have additional terms g_1, g_2 on the right hand side, as showed below,

$$-2\nu_c \mathbf{n}_{cm} \cdot \mathbb{D}(\mathbf{u}_c)\mathbf{n}_{cm} + P_c + \frac{1}{2}\rho_0|\mathbf{u}_c|^2 = P_m + g_1, \quad \text{on } \Gamma_{cm}, \tag{4.9}$$

$$-\tau_i \cdot \mathbb{D}(\mathbf{u}_c)\mathbf{n}_{cm} = \frac{\alpha_{BJSJ}}{2\sqrt{\mathrm{trace}(\Pi)}}\tau_i \cdot \mathbf{u}_c + g_2, \quad i = 1, \ldots, d-1, \text{on } \Gamma_{cm}, \tag{4.10}$$

where

$$g_1 = \frac{\rho_0}{2}e^{-2t}\sin^2(2\pi x), \qquad g_2 = -e^{-t}\left(\pi\cos(2\pi x) + \frac{\pi}{4}\sin^2(\pi x)\right). \tag{4.11}$$

Now we can start our experiment with the initial data set to be the exact solution above where $t = 0$, and we should calculate the relative error of the numerical solution with respect to the exact solution at $t = \mathcal{T} = 1$. In order to separate the convergence orders of both τ and h, we make separate experiments for $\tau = h$ and $\tau = h^3$. We also run the convergence tests for both $\mathbf{F} = \mathbf{F}^k$ and $\mathbf{F} = \mathbf{F}^{k+1}$ respectively. The experiment results are showed in Table 2-5.

Comparing the numerical results in the experiment A1 with those in A2, we can see that, when $\mathbf{F} = \mathbf{F}^k$, $P_c, P_m, \varphi, \mathrm{T}, U_c, U_m$ are all of first order in time, while the finite element of velocity and pressure $(\mathbf{u}, P)$ is set

to be (P2,P1) elements and φ, T are set to be P1 elements. Similar results can be obtained when $\mathbf{F} = \mathbf{F}^{k+1}$ by comparing the data in the experiments B1 and B2.

$\tau = h$	h		1/8	1/16	1/32	1/64	1/128
P_c, P_m : P1 element.	P_m	L^2 error	5.14109E-01	3.44479E-01	1.94682E-01	1.03525E-01	5.35046E-02
		Order		0.57766	0.82330	0.91114	0.95224
	P_c	L^2 error	6.14029E-01	3.98281E-01	2.17864E-01	1.12533E-01	5.70615E-02
		Order		0.62452	0.87036	0.95308	0.97976
φ, T : P1 element.	φ	L^2 error	1.06701	6.18081E-01	3.40457E-01	1.79831E-01	9.25595E-02
		Order		0.78771	0.86032	0.92083	0.95819
	T	L^2 error	8.85859E-02	4.94954E-02	2.62929E-02	1.36469E-02	6.96698E-03
		Order		0.83978	0.91262	0.94610	0.96997
T, U_c, U_m : P2 element.	$\mathbf{u}_c$	L^2 error	2.23059E-02	9.96694E-03	4.78455E-03	2.51573E-03	1.32212E-03
		Order		1.16220	1.05877	0.92741	0.92812
	$\mathbf{u}_m$	L^2 error	2.86016E-01	1.20892E-01	5.4497E-02	2.61285E-02	1.28782E-02
		Order		1.24238	1.14947	1.06055	1.02069

Table 2: Convergence test A1 where $T_0 = 0$, $T = 1$, $\tau = h$ and $\mathbf{F} = \mathbf{F}^k$.

4.2 Stability

In this section we numerically validate that the numerical methods satisfy discrete energy laws. The domain is given as $\Omega_m = [0,1] \times [0,1]$, $\Omega_c = [0,1] \times [-1,0]$, $\Omega = \Omega_m \cup \Omega_c = [0,1] \times [-1,1]$, $\Gamma_{cm} = [0,1] \times \{0\}$. The parameters in the PDE system are set as in Table 6. The initial conditions are $\varphi_0 = 0.2 + 0.4y$, $\mathrm{T}_0 = -xy$, and

$$\mathbf{u}_j(0) = \begin{pmatrix} -\frac{1}{2}\sin^2(\pi x)\sin(\pi(y+1)) \\ \sin(2\pi x)\sin^2(\frac{\pi(y+1)}{2}) \end{pmatrix}, \quad (x,y) \in \Omega_j,\ j \in \{c,m\}, \tag{4.12}$$

which satisfies $\nabla \cdot \mathbf{u}_0 = 0$. We take the mesh size $h = \frac{1}{64}$ and the time step $\tau = \frac{1}{64}$. We let the constant A to be either 10 or 100 in different tests in order to demonstrate the necessity of the condition (2.23). The numerical results for both $\mathbf{F} = \mathbf{F}^k$ and $\mathbf{F} = \mathbf{F}^{k+1}$ are shown in Fig. 2 (non-decay) and Fig. 3 (decay), respectively. Note that the discrete energy for the case $\mathbf{F} = \mathbf{F}^k$ is $\widetilde{\mathcal{E}}_A^k$, while the one for $\mathbf{F} = \mathbf{F}^{k+1}$ is $\mathcal{E}_A^k$. Observe that the discrete energy curves for $\mathbf{F} = \mathbf{F}^k$ and $\mathbf{F} = \mathbf{F}^{k+1}$ in both figures are almost identical

$\tau = h^3$	h		1/4	1/8	1/16	1/32	1/64
P_c, P_m : P1 element.	P_m	L^2 error	1.68465E-01	5.36559E-02	1.58287E-02	4.20343E-03	1.07305E-03
		Order		1.65064	1.76119	1.91290	1.96985
	P_c	L^2 error	3.12905E-01	7.542E-02	1.79264E-02	4.41531E-03	1.10148E-03
		Order		2.05271	2.07286	2.02150	2.00307
φ, T : P1 element.	φ	L^2 error	2.72186E-01	6.0609E-02	1.65777E-02	4.36422E-03	1.11381E-03
		Order		2.16699	1.87029	1.92545	1.97022
	T	L^2 error	2.84411E-02	6.27661E-03	1.48027E-03	3.62503E-04	9.01073E-05
		Order		2.17992	2.08413	2.02980	2.00828
U_c, U_m : P2 element.	$\mathbf{u}_c$	L^2 error	1.49899E-02	2.46298E-03	4.67624E-04	9.78403E-05	2.30435E-05
		Order		2.60551	2.39698	2.25685	2.08607
	$\mathbf{u}_m$	L^2 error	5.65454E-01	2.30529E-01	7.28347E-02	2.16234E-02	6.51941E-03
		Order		1.29446	1.66225	1.75203	1.72978

Table 3: Convergence test A2 where $T_0 = 0$, $T = 1$, $\tau = h^3$ and $\mathbf{F} = \mathbf{F}^k$.

$\tau = h$	h		1/8	1/16	1/32	1/64	1/128
P_c, P_m : P1 element.	P_m	L^2 error	5.14864E-01	3.44618E-01	1.94666E-01	1.035E-01	5.34892E-02
		Order		0.57919	0.82400	0.91137	0.95231
	P_c	L^2 error	6.08379E-01	3.95556E-01	2.16468E-01	1.1184E-01	5.67197E-02
		Order		0.62109	0.86973	0.95272	0.97951
φ, T : P1 element.	φ	L^2 error	1.06538	6.1707E-01	3.39933E-01	1.79575E-01	9.24359E-02
		Order		0.78786	0.86018	0.92066	0.95806
	T	L^2 error	8.86183E-02	4.94925E-02	2.6292E-02	1.36471E-02	6.96733E-03
		Order		0.84039	0.91259	0.94603	0.96992
U_c, U_m : P2 element.	$\mathbf{u}_c$	L^2 error	2.41098E-02	1.0395E-02	4.68559E-03	2.36767E-03	1.22548E-03
		Order		1.21373	1.14959	0.98476	0.95012
	$\mathbf{u}_m$	L^2 error	2.86063E-01	1.20653E-01	5.4234E-02	2.59563E-02	1.27824E-02
		Order		1.24547	1.15359	1.06311	1.02193

Table 4: Convergence test B1 where $T_0 = 0$, $T = 1$, $\tau = h$ and $\mathbf{F} = \mathbf{F}^{k+1}$.

thanks to the smallness of τ, $\bar{c}$ and α.

$\tau = h^3$	h		1/4	1/8	1/16	1/32	1/64
P_c, P_m : P1 element.	P_m	L^2 error	1.68303E-01	5.36625E-02	1.583E-02	4.20359E-03	1.07307E-03
		Order		1.64907	1.76125	1.91297	1.96988
	P_c	L^2 error	3.12831E-01	7.54368E-02	1.79284E-02	4.41556E-03	1.10152E-03
		Order		2.05204	2.07302	2.02158	2.00310
φ, T : P1 element.	φ	L^2 error	2.72286E-01	6.06491E-02	1.65832E-02	4.3649E-03	1.11389E-03
		Order		2.16656	1.87076	1.92570	1.97034
	T	L^2 error	2.84537E-02	6.27789E-03	1.48044E-03	3.62525E-04	9.011E-05
		Order		2.18026	2.08425	2.02987	2.00832
U_c, U_m : P2 element.	$\mathbf{u}_c$	L^2 error	1.51309E-02	2.45832E-03	4.66922E-04	9.78889E-05	2.30651E-05
		Order		2.62175	2.39642	2.25396	2.08543
	$\mathbf{u}_m$	L^2 error	5.65455E-01	2.30532E-01	7.2835E-02	2.16234E-02	6.51941E-03
		Order		1.29445	1.66226	1.75204	1.72978

Table 5: Convergence test B2 where $T_0 = 0$, $T = 1$, $\tau = h^3$ and $\mathbf{F} = \mathbf{F}^{k+1}$.

PDE parameters	α	κ	ρ_0	χ	ν_c	ν_m	Π	M(Mobility)	γ	ϵ	α_{BJSJ}	β	g
Value in test	0.5	$1e^{-3}$	1	1	0.1	0.1	$0.1\mathbb{I}_2$	0.1	0.1	0.1	$\sqrt{0.1}$	1	10

Table 6: Parameters in the discrete energy experiments. $\mathbb{I}_2$ represents the two-dimensional unit matrix.

4.3 Buoyancy-driven flow

In this numerical experiment we set $\Omega_m = [0,2] \times [0,0.5]$, $\Omega_c = [0,2] \times [-0.5,0]$, $\Omega = \Omega_m \cup \Omega_c = [0,2] \times [-0.5,0.5]$, $\Gamma_{cm} = [0,2] \times \{0\}$. The discrete parameters τ, h are set to be $\frac{1}{128}$ identically. The parameters in the PDE system are set as in Table 7.

κ	ρ_0	χ	ν_c	ν_m	Π	M(Mobility)	γ	ϵ	α_{BJSJ}	β	α	g
$1.1e^{-4}$	1	0.125	8.9e-7	8.9e-7	$0.001 \times \mathbb{I}_2$	$\epsilon\sqrt{(1-\varphi^2)^2+\epsilon^2}$	0.001	0.02	0.1	10	0.05	10

Table 7: Parameters in thermal conduction experiment. $\mathbb{I}_2$ represents the two-dimensional unit matrix.

We choose the initial data as $\mathbf{u}_0 = 0$, φ_0 to be a random function with uniform distribution in $[-1,1]$, and $\mathrm{T}_0 = -2y$. Additionally, for all $t \geq 0$ we set constant hot bottom and cold top to this system, i.e. $\mathrm{T}\big|_{y=-0.5} \equiv 1$ and $\mathrm{T}\big|_{y=0.5} \equiv -1$ as Dirichlet boundary condition, while T is endowed with Neumann condition on the rest

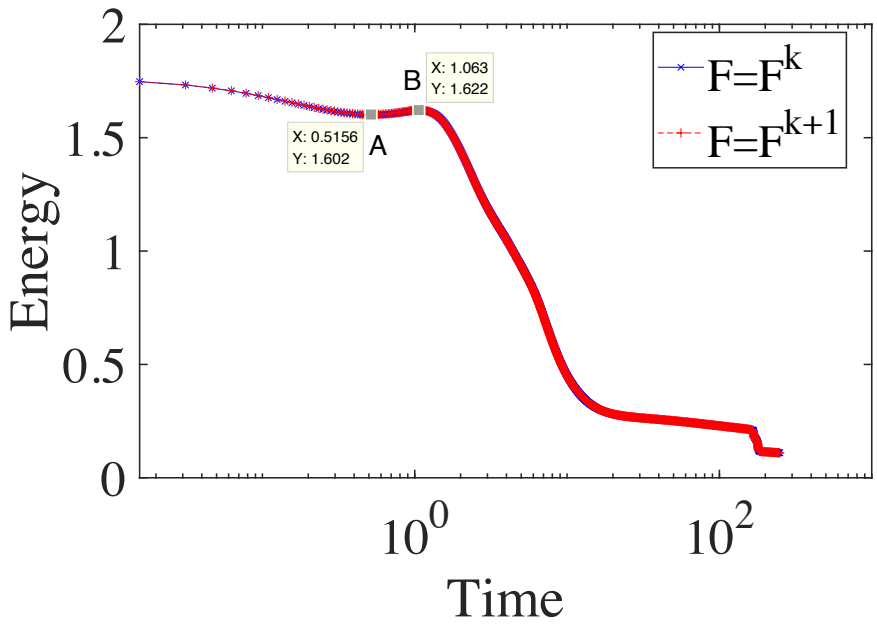

Fig. 2: Evolution of discrete energy with the constant $A = 10$. The two energy curves are almost identical. Point A (0.5156,1.602) and Point B (1.063,1.622) show that the discrete energy is non-decaying.

of the boundary. The setup of the boundary conditions leads to the convection phenomenon. We run the numerical experiment for sufficiently long time so that steady convection cells (Benard Cells) are observable. The snapshots of velocity functions are shown in Fig. 4,5, representing the numerical scheme with $\mathbf{F} = \mathbf{F}^k$ and $\mathbf{F} = \mathbf{F}^{k+1}$ respectively.

We see from Figure 4 that there are initially two convection cells extending throughout the whole domain (Fig. 4(a)). As it progresses, the fluid in the lower sub-domain governed by the Navier-Stokes equations becomes "turbulent" and breaks the big convection cells (Fig. 4(b)). Afterwards several small convection cells appear in the upper sub-domain (porous media), cf. Fig. 4(c). In long time, the convection cells are mostly confined in porous media and become steady. Similar phenomena are observed in Fig. 5.

5 Conclusions

In this article, we propose the Cahn-Hilliard-Navier-Stokes-Darcy-Boussinesq (CHNSDB) system for thermal convection of two-phase flows in a fluid layer overlying a porous medium. The physical model satisfies an energy law, and encompasses four processes: the phase field model governed by the Cahn-

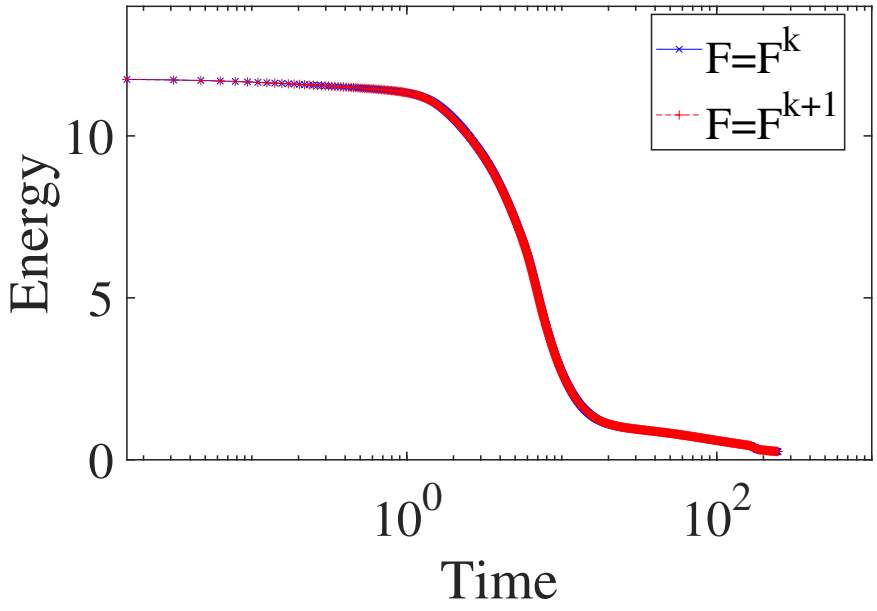

Fig. 3: Evolution of discrete energy with the constant $A = 100$. The two energy curves are visibly identical and monotonically deceasing.

Hilliard equations, the thermal convection governed by the heat equation, fluid systems governed by the Darcy equations in porous media and the Navier-Stokes equations in free flow. We design uniquely solvable algorithms that preserve the underlying energy law. Moreover, our algorithms fully decouple the Cahn-Hilliard equations, the heat equation, the Navier-Stokes equations and the Darcy equations, so that each sub-system can be computed independently at each time step. Several numerical experiments are performed to gauge the accuracy and robustness of the proposed algorithms. The error estimates of the numerical schemes will be pursued in a future work.

References

1. Henri Bénard. Les tourbillons cellulaire dans nappe liquide transportant de la chaleur purconvections en regime permanent. Rev. Gen. Sci. Pures Appl. Bull. Assoc., 11:1309–1328, 1900.
2. Yanzhao Cao, Max Gunzburger, Fei Hua, and Xiaoming Wang. Coupled Stokes-Darcy model with Beavers-Joseph interface boundary condition. Commun. Math. Sci., 8(1):1–25, 2010.

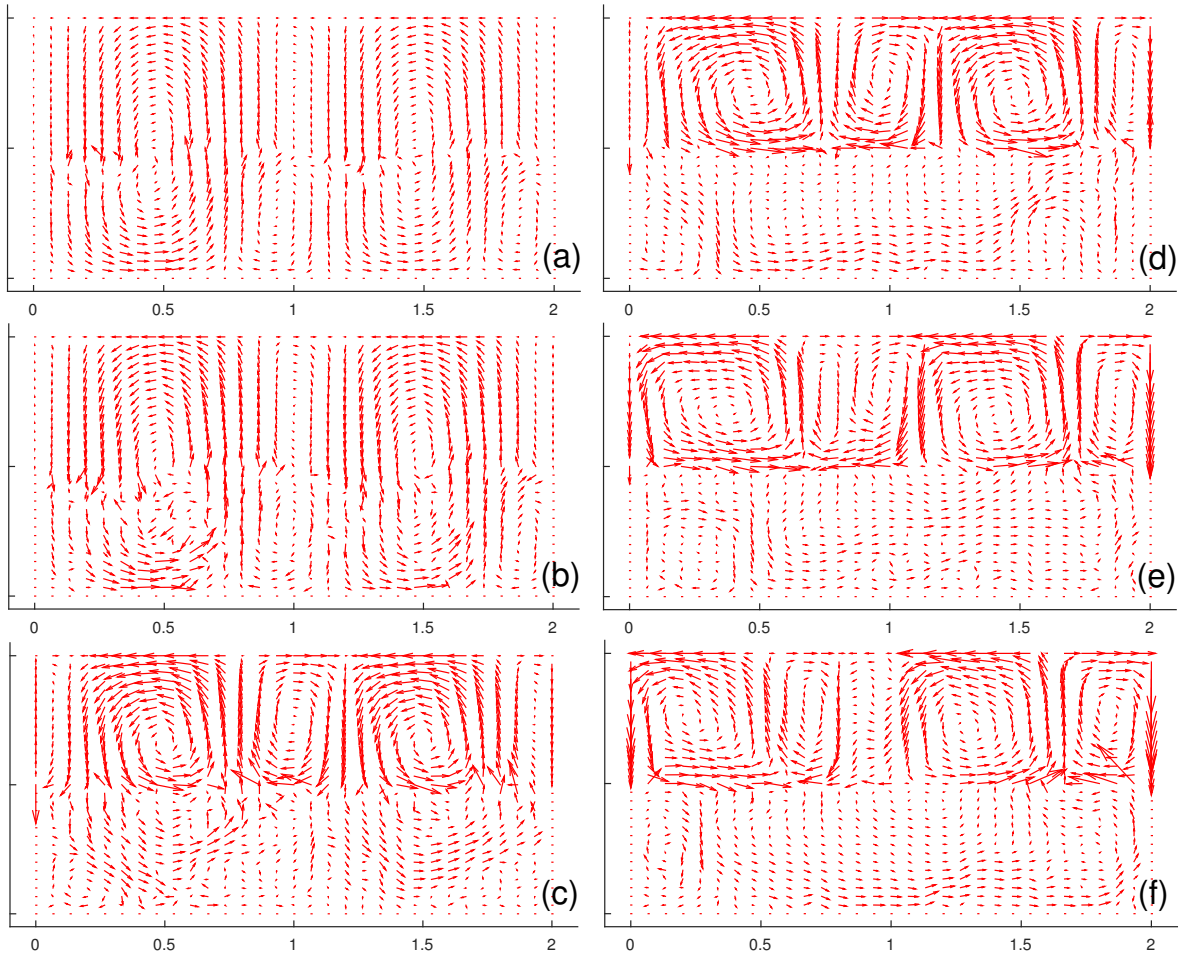

Fig. 4: The snapshots of velocity field $\mathbf{u}_h$ for $\mathbf{F} = \mathbf{F}^k$. (a) $t = 0.477$. (b) $t = 0.789$. (c) $t = 3.914$. (d) $t = 15.633$. (e) $t = 39.070$. (f) $t = 60.945$.

3. M. Bayani Cardenas. Hyporheic zone hydrologic science: A historical account of its emergence and a prospectus. Water Resources Research, 51(5):3601–3616, 2015.

4. Andrew M. Stuart Charles M. Elliott. The global dynamics of discrete semilinear parabolic equations. SIAM J. Numer. Anal., 30(6):1622–1663, 1993.

5. Jie Chen, Shuyu Sun, and Xiao-Ping Wang. A numerical method for a model of two-phase flow in a coupled free flow and porous media system. J. Comput. Phys., 268:1–16, 2014.

6. Nan Chen, Max Gunzburger, and Xiaoming Wang. Asymptotic analysis of the differences between the Stokes-Darcy system with different interface conditions and the Stokes-Brinkman system. J. Math. Anal. Appl., 368(2):658–676, 2010.

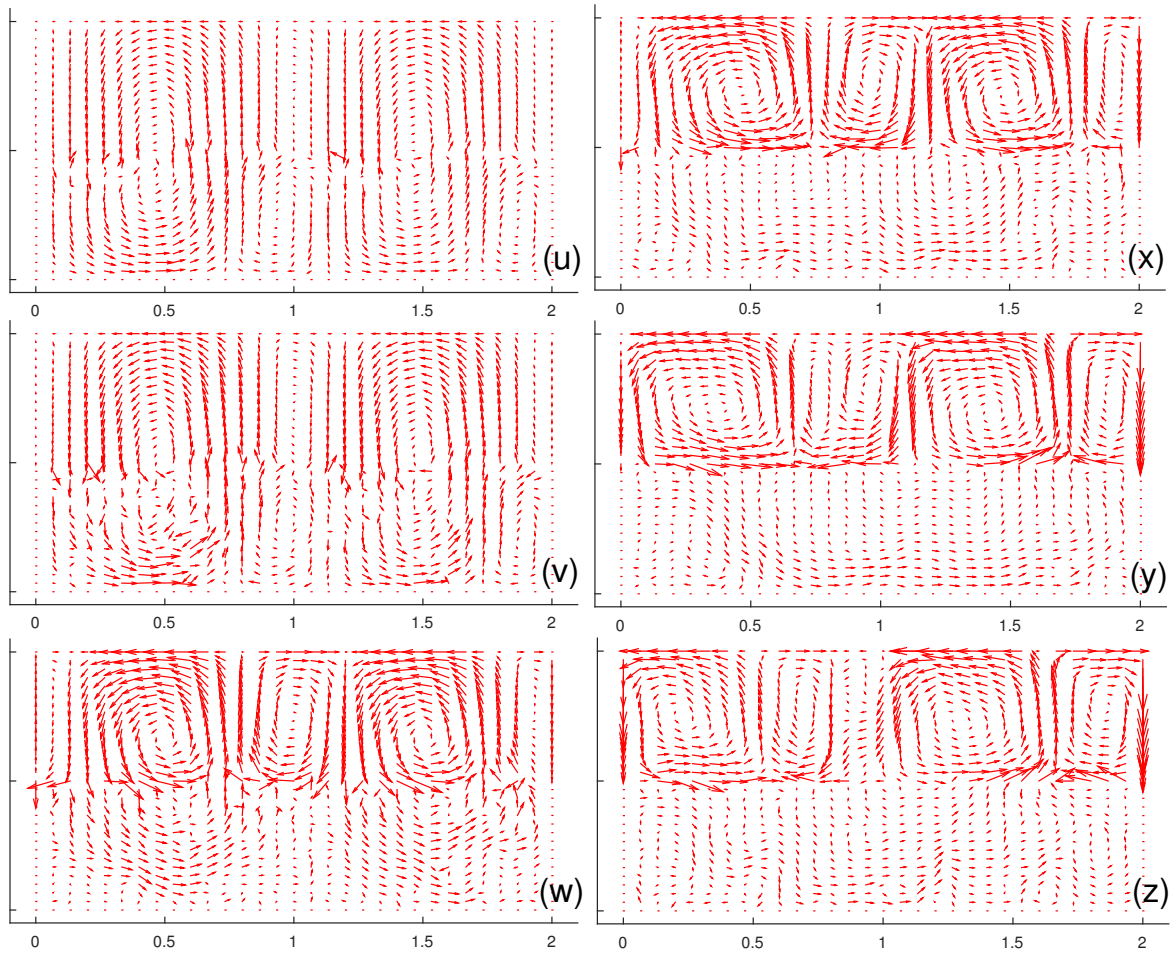

Fig. 5: The vector snapshot of velocity $\mathbf{u}_h$ for $\mathbf{F} = \mathbf{F}^{k+1}$. (u) is for $t = 0.477$. (v) is for $t = 0.789$. (w) is for $t = 3.914$. (x) is for $t = 15.633$. (y) is for $t = 39.070$. (z) is for $t = 60.945$.

7. Wenbin Chen, Max Gunzburger, Fei Hua, and Xiaoming Wang. A parallel robin-robin domain decomposition method for the stokes-darcy system. SIAM JOURNAL ON NUMERICAL ANALYSIS, 49(3):1064–1084, 2011.

8. Wenbin Chen, Max Gunzburger, Dong Sun, and Xiaoming Wang. Efficient and long-time accurate second-order methods for the Stokes-Darcy system. SIAM J. Numer. Anal., 51(5):2563–2584, 2013.

9. Wenbin Chen, Daozhi Han, and Xiaoming Wang. Uniquely solvable and energy stable decoupled numerical schemes for the Cahn-Hilliard-Stokes-Darcy system for two-phase flows in karstic geometry. Numer. Math., 137(1):229–255, 2017.

10. Alexandre Joel Chorin. Numerical solution of the Navier-Stokes equations. Math. Comp., 22:745–762, 1968.

11. Amanda E. Diegel, Cheng Wang, Xiaoming Wang, and Steven M. Wise. Convergence analysis and error estimates for a second order accurate finite element method for the Cahn-Hilliard-Navier-Stokes system. Numer. Math., 137(3):495–534, 2017.

12. Marco Discacciati and Alfio Quarteroni. Navier-Stokes/Darcy coupling: modeling, analysis, and numerical approximation. Rev. Mat. Complut., 22(2):315–426, 2009.

13. David J. Eyre. Unconditionally gradient stable time marching the Cahn-Hilliard equation. In Computational and mathematical models of microstructural evolution (San Francisco, CA, 1998), volume 529 of Mater. Res. Soc. Sympos. Proc., pages 39–46. MRS, Warrendale, PA, 1998.

14. Xiaobing Feng and Steven Wise. Analysis of a Darcy-Cahn-Hilliard diffuse interface model for the Hele-Shaw flow and its fully discrete finite element approximation. SIAM J. Numer. Anal., 50(3):1320–1343, 2012.

15. Giordano Tierra Francisco Guillén-González. On linear schemes for a Cahn-Hilliard diffuse interface model. J. Comput. Phys., 234:140–171, 2013.

16. Vivette Girault and Pierre-Arnaud Raviart. Finite element methods for Navier-Stokes equations: theory and algorithms volume 5. Springer Science & Business Media, 2012.

17. Vivette Girault and Béatrice Rivière. DG approximation of coupled Navier-Stokes and Darcy equations by Beaver-Joseph-Saffman interface condition. SIAM J. Numer. Anal., 47(3):2052–2089, 2009.

18. Karl Glasner and Saulo Orizaga. Improving the accuracy of convexity splitting methods for gradient flow equations. J. Comput. Phys., 315:52–64, 2016.

19. J.G. Gluyas and R.E. Swarbrick. Petroleum Geology. Blackwell publishing, 2004.

20. Yuezheng Gong, Jia Zhao, and Qi Wang. Arbitrarily high-order unconditionally energy stable schemes for thermodynamically consistent gradient flow models. SIAM J. Sci. Comput., 42(1):B135–B156, 2020.

21. Yuezheng Gong, Jia Zhao, Xiaogang Yang, and Qi Wang. Fully discrete second-order linear schemes for hydrodynamic phase field models of binary viscous fluid flows with variable densities. SIAM J. Sci. Comput., 40(1):B138–B167, 2018.

22. Zhenlin Guo and Ping Lin. A thermodynamically consistent phase-field model for two-phase flows with thermocapillary effects. J. Fluid Mech., 766:226–271, 2015.

23. Zhenlin Guo, Ping Lin, John Lowengrub, and Steven Wise. Mass conservative and energy stable finite difference methods for the quasi-incompressible Navier-Stokes-Cahn-Hilliard system: primitive variable and projection-type schemes. Comput. Methods Appl. Mech. Engrg., 326:144–174, 2017.

24. Daozhi Han. A decoupled unconditionally stable numerical scheme for the Cahn-Hilliard-Hele-Shaw system. J. Sci. Comput., 66(3):1102–1121, 2016.

25. Daozhi Han, Dong Sun, and Xiaoming Wang. Two-phase flows in karstic geometry. Mathematical Methods in the Applied Sciences, 37(18):3048–3063, 2014.

26. Daozhi Han and Xiaoming Wang. A second order in time, uniquely solvable, unconditionally stable numerical scheme for Cahn–Hilliard–Navier–Stokes equation. J. Comput. Phys., 290:139–156, 2015.

27. Daozhi Han, Xiaoming Wang, and Hao Wu. Existence and uniqueness of global weak solutions to a Cahn–Hilliard–Stokes–Darcy system for two phase incompressible flows in karstic geometry. Journal of Differential Equations, 257(10):3887–3933, 2014.

28. Qiaolin He, Roland Glowinski, and Xiao-Ping Wang. A least-squares/finite element method for the numerical solution of the Navier-Stokes-Cahn-Hilliard system modeling the motion of the contact line. J. Comput. Phys., 230(12):4991–5009, 2011.

29. Frédéric Hecht. New development in freefem++. Journal of numerical mathematics, 20(3-4):251–266, 2012.

30. Antony A. Hill and Brian Straughan. Global stability for thermal convection in a fluid overlying a highly porous material. Proc. R. Soc. Lond. Ser. A Math. Phys. Eng. Sci., 465(2101):207–217, 2009.

31. David Kay, Vanessa Styles, and Richard Welford. Finite element approximation of a Cahn-Hilliard-Navier-Stokes system. Interfaces Free Bound, 10(1):15–43, 2008.

32. Junseok Kim, Kyungkeun Kang, and John Lowengrub. Conservative multigrid methods for Cahn-Hilliard fluids. J. Comput. Phys., 193(2):511–543, 2004.

33. William J. Layton, Friedhelm Schieweck, and Ivan Yotov. Coupling fluid flow with porous media flow. SIAM J. Numer. Anal., 40(6):2195–2218 (2003), 2002.

34. Sebastian Minjeaud. An unconditionally stable uncoupled scheme for a triphasic Cahn-Hilliard/Navier-Stokes model. Numer. Methods Partial Differential Equations, 29(2):584–618, 2013.

35. Jie Shen. Modeling and numerical approximation of two-phase incompressible flows by a phase-field approach. In Multiscale modeling and analysis for materials simulation, pages 147–195. World Scientific, 2012.

36. Jie Shen, Cheng Wang, Xiaoming Wang, and Steven M. Wise. Second-order convex splitting schemes for gradient flows with Ehrlich-Schwoebel type energy: application to thin film epitaxy. SIAM J. Numer. Anal., 50(1):105–125, 2012.

37. Jie Shen, Jie Xu, and Jiang Yang. The scalar auxiliary variable (SAV) approach for gradient flows. J. Comput. Phys., 353:407–416, 2018.

38. Jie Shen, Jie Xu, and Jiang Yang. A new class of efficient and robust energy stable schemes for gradient flows. SIAM Rev., 61(3):474–506, 2019.

39. Jie Shen and Xiaofeng Yang. Numerical approximations of Allen-Cahn and Cahn-Hilliard equations. Discrete Contin. Dyn. Syst., 28(4):1669–1691, 2010.

40. Jie Shen and Xiaofeng Yang. Decoupled, energy stable schemes for phase-field models of two-phase incompressible flows. SIAM J. Numer. Anal., 53(1):279–296, 2015.

41. Charles J. Taylor and Earl A. Greene. Quantitative Approaches in Characterizing Karst Aquifers. 2001. Water Resources Investigations Report 01-4011.

42. Roger Temam. Une méthode d'approximation de la solution des équations de Navier-Stokes. Bull. Soc. Math. France, 96:115–152, 1968.

43. Klaus Tüber, David Pócza, and Christopher Hebling. Visualization of water buildup in the cathode of a transparent pem fuel cell. Journal of power sources, 124(2):403–414, 2003.

44. Steven Wise. Unconditionally stable finite difference, nonlinear multigrid simulation of the Cahn-Hilliard-Hele-Shaw system of equations. J. Sci. Comput., 44(1):38–68, 2010.

45. Xiaofeng Yang and Lili Ju. Linear and unconditionally energy stable schemes for the binary fluid-surfactant phase field model. Comput. Methods Appl. Mech. Engrg., 318:1005–1029, 2017.

46. Xiaofeng Yang, Jia Zhao, and Qi Wang. Numerical approximations for the molecular beam epitaxial growth model based on the invariant energy quadratization method. J. Comput. Phys., 333:104–127, 2017.

47. Jia Zhao, Xiaofeng Yang, Yuezheng Gong, and Qi Wang. A novel linear second order unconditionally energy stable scheme for a hydrodynamic **Q**-tensor model of liquid crystals. Comput. Methods Appl. Mech. Engrg., 318:803–825, 2017.